

**A Comparative Study of Empirical, Statistical, and Analytical Models
for Landslide Susceptibility in Kullu District, Himachal Pradesh**

MAJOR PROJECT I REPORT

A Dissertation Submitted

In Partial Fulfillment of the Requirements for the Degree of

MASTERS OF TECHNOLOGY

IN

GEOTECHNICAL ENGINEERING

BY

DHIREN SAGAR

(2K23/GTE/09)

Under the Supervision of

Prof. RAJU SARKAR

Professor

Delhi Technological University



Department of Civil Engineering
DELHI TECHNOLOGICAL UNIVERSITY
(Formerly Delhi College of Engineering)
Shahbad Daulatpur, Main Bawana Road, Delhi-110042

MAY 2025

**A Comparative Study of Empirical, Statistical, and Analytical Models
for Landslide Susceptibility in Kullu District, Himachal Pradesh**

MAJOR PROJECT I REPORT

A Dissertation Submitted
In Partial Fulfillment of the Requirements for the Degree of

MASTERS OF TECHNOLOGY

IN
GEOTECHNICAL ENGINEERING
BY

DHIREN SAGAR
(2K23/GTE/09)

Under the Supervision of

Prof. RAJU SARKAR
Professor
Delhi Technological University



Department of Civil Engineering
DELHI TECHNOLOGICAL UNIVERSITY
(Formerly Delhi College of Engineering)
Shahbad Daultpur, Main Bawana Road, Delhi-110042

MAY 2025



DELHI TECHNOLOGICAL UNIVERSITY
(Formerly Delhi College of Engineering)
Shahbad Daulatpur, Main Bawana Road, Delhi-110042

CANDIDATE'S DECLARATION

I, **DHIREN SAGAR**, M. Tech (Geotechnical Engineering) student, having **Roll no: 2K23/GTE/09**, hereby certify that the work which is being presented in the dissertation entitled "**A Comparative Study of Empirical, Statistical, and Analytical Models for Landslide Susceptibility in Kullu District, Himachal Pradesh**" in partial fulfillment of the requirements for the award of the Degree of **Master Of Technology in Geotechnical Engineering**, submitted in the **Department of Civil Engineering, Delhi Technological University**, Delhi Technological University is an authentic record of my work carried out under the supervision of **Prof. Raju Sarkar**, Professor, Department of Civil Engineering, Delhi Technological University, Delhi.

I have not submitted the matter presented in this dissertation for the award of any other degree from this or any other institute.

(DHIREN SAGAR)

This is to certify that the student has incorporated all the corrections suggested by the examiners in the thesis and that the statement made by the candidate is correct to the best of our knowledge.

Prof. RAJU SARKAR
(Supervisor)

Place: Delhi, Date:

(Signature of Examiner)



DELHI TECHNOLOGICAL UNIVERSITY
(Formerly Delhi College of Engineering)
Shahbad Daulatpur, Main Bawana Road, Delhi-110042

CERTIFICATE BY THE SUPERVISOR(s)

Certified that **DHIREN SAGAR (2K23/GTE/09)** has carried out his research work presented in this thesis entitled “**A Comparative Study of Empirical, Statistical, and Analytical Models for Landslide Susceptibility in Kullu District, Himachal Pradesh**” for the award of the Degree of **Master of Technology in Geotechnical Engineering** from the Department of Civil Engineering, Delhi Technological University, Delhi, under our supervision. The thesis embodies the results of the original work, and the student himself carries out studies. The contents of the thesis do not form the basis for the award of any degree to the candidate or anybody else from this or any other University/Institution.

Prof. RAJU SARKAR
(Supervisor)

Professor
Delhi Technological University

Place: Delhi,

Date:

ABSTRACT

Kullu district of Himachal Pradesh, India, is highly susceptible to landslides due to its rugged terrain, complex geological conditions, and heavy seasonal rainfall. This study evaluates and compares three different modeling approaches for landslide susceptibility mapping—empirical (Frequency Ratio), statistical (Shannon Entropy), and analytical (Analytical Hierarchy Process)—to determine the most effective technique for predicting landslide-prone areas.

A comprehensive landslide inventory comprising 428 landslide events and ten Landslide Conditioning Factors (LCFs), including slope, elevation, aspect, lithology, and proximity to streams, was used to develop susceptibility maps. The Frequency Ratio (FR) model demonstrated the highest predictive accuracy with an AUC value of 0.738, followed closely by the Shannon Entropy (SE) model (AUC = 0.735). The AHP model (AUC = 0.635) exhibited lower predictive performance, suggesting limitations in its weighting scheme for this region. Validation techniques, including AUC-ROC analysis and Success-Prediction Rate curves, confirmed the reliability and generalizability of the models.

The findings emphasize the effectiveness of statistical and empirical models over analytical methods for landslide susceptibility assessment in mountainous terrains. The generated susceptibility maps are a valuable tool for disaster risk management, infrastructure planning, and sustainable development in the Kullu district. This research improves landslide prediction methodologies and supports targeted mitigation strategies for high-risk regions.

ACKNOWLEDGEMENT

I, **DHIREN SAGAR**, would like to express my deepest gratitude to all those who have given unforgettable contributions to the successful contribution of this thesis.

I want to thank Prof. Prateek Sharma, Vice Chancellor, for providing all the facilities and helping carry out this project. I thank **Prof. Raju Sarkar**, Associate Dean, for the stimulus provided.

I am extremely grateful to **Dr. K. C. Tiwari**, Professor and Head of the Department of Civil Engineering, for the encouragement and support provided during the project work.

I sincerely thank the coordinator, **Dr. Ashok Kumar Gupta**, Professor, for his valuable suggestions for improvement during project reviews.

I acknowledge with deep gratitude the valuable guidance, encouragement, and suggestions from my project guide, **Prof. Raju Sarkar**, Professor, who has been a constant source of inspiration throughout this project.

I would also like to take this opportunity to thank all the faculty members and non-teaching staff members in the Department of Civil Engineering for their direct and indirect help rendered during the course of the project work.

Lastly, I would like to express my immense gratitude towards god. I wouldn't have been what I am today without his/her blessing. Please, god, always keep me on the list of your much-loved children.

DHIREN SAGAR
2K23/GTE/09
DTU DELHI 110042

TABLE OF CONTENTS

Chapter no.	Title	Page no.
	Candidate's Declaration	I
	Certificate by the supervisor	II
	Abstract	III
	Acknowledgment	IV
	List of Tables	VIII
	List of Figures	IX
1	Introduction	1
2	Literature Review	3
3	Methodology	7
4	Data Source	8
5	Study Area: Kullu Himachal Pradesh	9
6	Landslide Inventory Map	10
7	Landslide conditioning factors	11
	7.1 Slope	11
	7.2 Aspect	12
	7.3 Distance From Stream	13
	7.4 Curvature	14
	7.5 Elevation	15
	7.6 Lithology	16
	7.7 Hillshade	17

	7.8 Contour	18
	7.9 Topographic Wetness Index	19
	7.10 Roughness	20
8	Empirical Technique	21
	8.1 Introduction	21
	8.2 Formula	21
	8.3 Outcome	21
	8.4 Application	22
	8.5 Advantage	22
9	Statistical Technique	28
	9.1 Introduction	28
	9.2 Formula	28
	9.3 Outcome	29
	9.4 Application	29
	9.5 Advantage	29
10	Analytical Technique	37
	10.1 Introduction	37
	10.2 Formula	37
	10.3 Outcome	38
	10.4 Application	38
	10.5 Advantage	38
11	Results	41
	11.1 Discussion	41
	11.2 Validation	45
12	Conclusion and Future Focus	47

12.1 Conclusion	47
12.2 Future Focus	47
Reference	49
Publication	54

LIST OF TABLES

Table Number	Title	Page No.
4.1	Data Source	8
8.1	Frequency Ratio Calculation	23
9.1	Shannon Entropy Calculation	31
10.1	AHP Matrix	39
10.2	CI Values	40

LIST OF FIGURES

Figure No.	Title	Page No.
3.1	Methodology	7
5.1	Study Area Map	9
6.1	Landslide Inventory Map	10
7.1	Slope	11
7.2	Aspect	12
7.3	Distance from stream	13
7.4	Curvature	14
7.5	Elevation	15
7.6	Lithology	16
7.7	Hillshade	17
7.8	Contour	18
7.9	TWI	19
7.10	Roughness	20
11.1	Susceptibility Map using AHP	42
11.2	Susceptibility Map using FR	43
11.3	Susceptibility Map using Shannon Entropy	44
11.4	Success Rate Curve	45
11.5	Prediction Rate Curve	46

CHAPTER 1

INTRODUCTION

The Kullu district of Himachal Pradesh, located in northern India, is renowned for its scenic landscapes but is also highly susceptible to landslides due to its steep terrain, complex geological formations, heavy monsoon rainfall, and increasing human activities such as construction and deforestation. Landslides pose significant threats to life, property, infrastructure, and the environment, making accurate susceptibility mapping crucial for disaster preparedness, risk reduction, and sustainable development.

Landslide Susceptibility Mapping (LSM) helps identify high-risk areas by analyzing various environmental, topographical, and geological factors. It is a vital tool for disaster management, infrastructure planning, and land-use regulation. Researchers have employed empirical, statistical, and analytical models to assess landslide-prone regions, each offering distinct advantages and limitations. This study evaluates three widely used methods:

- Empirical Model (Frequency Ratio - FR): Determines susceptibility based on the observed correlation between past landslide occurrences and Landslide Conditioning Factors (LCFs).
- Statistical Model (Shannon Entropy - SE): Measures the contribution of each LCF by analyzing its information gain in reducing uncertainty.
- Analytical Model (Analytical Hierarchy Process - AHP): Uses expert-driven pairwise comparisons to assign relative importance to LCFs.

The study area exhibits challenging topographical conditions, with elevations ranging from 1,200 m to over 6,000 m, deep valleys, and narrow gorges. Heavy monsoon rainfall, snowmelt, and human-induced slope modifications further increase landslide susceptibility. The research integrates a landslide inventory of 428 documented events and

ten LCFs, including slope, aspect, elevation, lithology, curvature, and distance from streams, derived using geospatial tools.

Findings indicate that the Frequency Ratio and Shannon Entropy models outperform the AHP model in predictive accuracy, as validated by AUC-ROC analysis. The FR model achieved the highest AUC value of 0.738, followed closely by the SE model (AUC = 0.735), while the AHP model exhibited a lower predictive performance (AUC = 0.635), suggesting limitations in its factor weighting. Success Rate and Prediction Rate curves further confirmed the reliability of the statistical-based approaches.

The study underscores the importance of data-driven and statistical models for landslide prediction in mountainous regions. The generated susceptibility maps provide valuable insights for disaster management, infrastructure development, and environmental protection. These findings contribute to enhancing geomorphological hazard assessment and support targeted mitigation strategies for landslide-prone areas in Kullu district.

CHAPTER 2

LITERATURE REVIEW

Badavath, N., Sahoo, S., & Samal, R. (2024). Landslide susceptibility mapping for West-Jaintia Hills district, Meghalaya. *Sāadhanā*. Highlights causative factors like rainfall, slope, and NDVI with 75% training and 25% testing.

Chen, W., Guo, C., Lin, F., Zhao, R., & Li, T. (2024). Exploring advanced machine learning techniques for landslide susceptibility mapping in Yanchuan County, China. *Earth Science Informatics*. The dataset comprises 311 landslide points with a training-to-validation ratio of 7:3.

Chen, Z., Tang, J., & Song, D. (2024). Modeling landslide susceptibility using alternating decision tree and support vector. *Terrestrial, Atmospheric and Oceanic Sciences*. Employs ROC analysis to test ADTree and SVM models.

Dorji, L., & Sarkar, R. (2024). Hydrological modeling using CN method and satellite images in the Barsa River Basin, Bhutan. *Springer Nature Singapore*. Highlights hydrological modeling for ungauged basins.

Gayen, A., & Haque, S. M. (2024). Gully erosion susceptibility using advanced machine learning method in Pathro River Basin, India. *Springer Nature Singapore*. This study evaluates susceptibility using SAGAGIS and ArcGIS tools with training (70%) and testing (30%) data splits.

Ha, H., Bui, Q. D., & Tran, D. T. (2024). Improving forecast performance of landslide susceptibility mapping using gradient boosting algorithms. *Environment, Development and Sustainability*. Uses ensemble gradient boosting methods for susceptibility forecasting.

Khatun, S., Saha, A., & Sarkar, R. (2024). Assessment of landslide vulnerability using statistical and machine learning methods in Uttarakhand, India. *Springer Nature Singapore*. Uses statistical tools for susceptibility modeling.

Lau, R., Seguí, C., Waterman, T., & Veveakis, M. (2024). Quantitative assessment of Interferometric Synthetic Aperture Radar (INSAR) for landslide monitoring and mitigation. *Springer Nature Singapore*. Employs RMSE for evaluating INSAR-based landslide assessments.

lv, J., Zhang, R., Shama, A., & Hong, R. (2024). Exploring the spatial patterns of landslide susceptibility assessment using interpretable Shapley method. *Journal of Environmental Management*. Conducts assessments using RF, SVM, and XGBoost models.

Pal, S., Saha, A., Gogoi, P., & Saha, S. (2024). An ensemble of J48 decision tree with AdaBoost and Bagging for flood susceptibility mapping in the Sundarbans of West Bengal, India. *Springer Nature Singapore*. Investigates flood mapping with validation metrics such as AUC and Kappa coefficients.

Paul, G. C., & Saha, S. (2024). Flood resilience assessment in Mayurakshi River Basin. *Springer Nature Singapore*. Focuses on resilience planning for flood-prone areas.

Pradhan, B., & Alamri, A. M. (2024). Advanced GIS applications in hazard and risk assessment. *Springer Nature Singapore*. Discusses GIS innovations for risk mapping.

Reddy, N. D. K., Gupta, A. K., & Sahu, A. K. (2024). Random Forest (RF) and Support Vector Machine (SVM) with Cat Swarm Optimization for soil liquefaction prediction. *Springer Nature Singapore*. Implements optimized RF and SVM for liquefaction analysis.

Roy, B., Gogoi, P., & Saha, S. (2024). Assessment of shifting of River Ganga along Malda district of West Bengal using satellite images. *Springer Nature Singapore*. Uses temporal satellite imagery to assess geomorphic changes.

Saha, A., Saha, S., & Sarkar, R. (2024). Novel ensemble of M5P and deep learning neural network for predicting landslide susceptibility: A cross-validation approach. *Springer Nature Singapore*. Focused on hybrid machine learning models with MAE and RMSE validation.

Saha, S., Saha, A., & Agarwal, A. (2024). Spatial flash flood modeling in the Beas River Basin of Himachal Pradesh, India. *Springer Nature Singapore*. Focuses on GIS-based machine learning for flood risk assessment.

Saha, S., Saha, A., Roy, B., Chaudhary, A., & Sarkar, R. (2024). Artificial neural network ensemble with a general linear model for modeling the landslide susceptibility in the Mirik region of West Bengal, India. *Springer Nature Singapore*. The study uses 373 landslide locations and multiple validation metrics, including ROC and RMSE.

Saha, S., & Sarkar, R. (2024). Measuring landslide susceptibility in Jakholi region of Garhwal Himalaya using Landsat images. *Springer Nature Singapore*. Combines statistical and machine learning ensembles for susceptibility.

Sameen, M. I., Sarkar, R., Pradhan, B., Drukpa, D., & Alamri, A. M. (2020). Landslide spatial modeling using unsupervised factor optimization and regularized greedy forests. *Computers & Geosciences*, 134, 104336. Focuses on spatial modeling with 952 landslide points using RGF.

Sarkar, R., & Sujeewon, B. C. (2024). Landslide susceptibility mapping using satellite images and GIS-based statistical approaches in part of Kullu district. *Springer Nature Singapore*. Evaluates GIS integration in susceptibility modeling.

Sarkar, R., Sujeewon, B. C., & Pawar, A. (2024). Landslide susceptibility mapping using satellite images in Himachal Pradesh, India. *Springer Nature Singapore*. Explores GIS-based satellite methods for accurate mapping.

Sharma, A., & Prakash, C. (2023). Impact assessment of road construction on landslide susceptibility in mountainous region using GIS-based statistical modeling. *Journal of the Geological Society of India*. Focused on road-induced landslide susceptibility in Mandi district.

Thapa, R., Sarkar, R., & Gupta, S. (2024). Geospatial study of river shifting and erosion-deposition in the River Damodar, West Bengal. *Springer Nature Singapore*. Analyzes geomorphological risks using geospatial tools.

Wei, Y., Qiu, H., Liu, Z., & Kamp, U. (2024). Refined and dynamic susceptibility assessment of landslides using InSAR and machine learning. *Geoscience Frontiers*. Integrates RF, LR, and GBDT for improved susceptibility assessment.

CHAPTER 3

METHODOLOGY

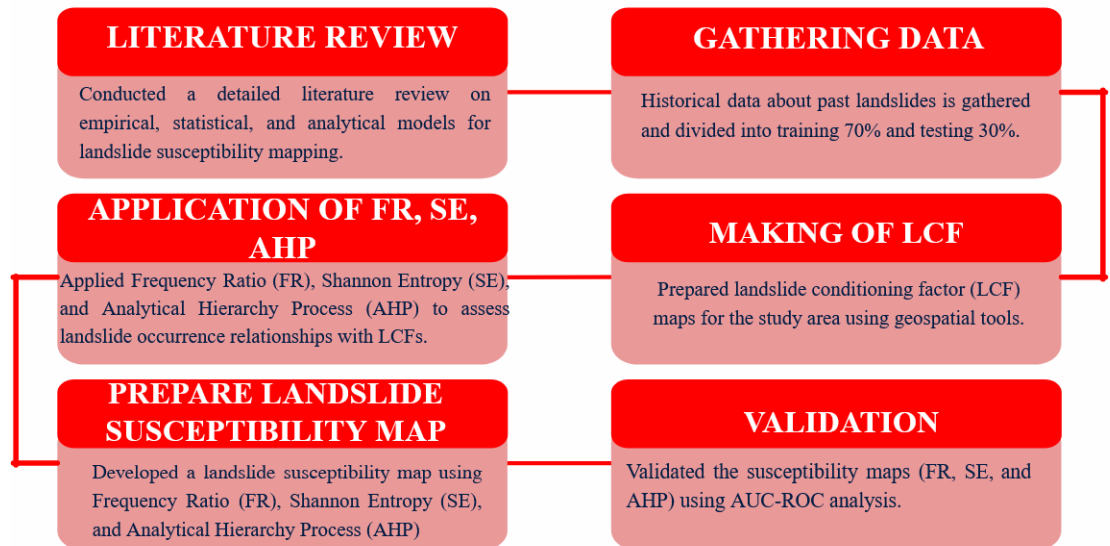


Figure 3. 1: METHODOLOGY

CHAPTER 4

DATA SOURCE

TABLE 4.1: DATA SOURCE

MAP	DATA SOURCE
INDIAN MAP	https://www.indianremotesensing.com/2017/01/Download-India-shapefile-with-kashmir.html
LANDSLIDE POINTS	https://bhukosh.gsi.gov.in/Bhukosh/Public
DISTRICT AND SUB-DISTRICT MAPS	https://esriindia1.maps.arcgis.com/home/item.html?id=b89de19caf b94ea38552a55eb5b2d13d
SLOPE, ASPECT, ROUGHNESS, TWI	https://opentopography.org/
DISTANCE FROM DRAINAGE	https://www.hydrosheds.org/products/hydrorivers#downloads
LITHOLOGY	https://certmapper.cr.usgs.gov/data/apps/world-maps/
CURVATURE, CONTOUR, HILLSHADE, ELEVATION	https://earthexplorer.usgs.gov/

CHAPTER 5

STUDY AREA: KULLU, HIMACHAL PRADESH

Kullu district is located in the state of Himachal Pradesh, in northern India. It lies between latitudes 31°20' to 32°25' N and longitudes 76°56' to 77°52' E. The district is part of the Western Himalayas and covers an area of approximately 5,503 square kilometers.

Kullu is characterized by a rugged and mountainous terrain, with altitudes ranging from 1,200 meters to over 6,000 meters above sea level. The district is known for its steep slopes, deep valleys, and narrow gorges, making it highly susceptible to landslides, particularly during the monsoon season.

The district experiences a temperate climate with significant rainfall during the monsoon season (July to September).

The region also receives heavy snowfall in higher altitudes during the winter. The average annual rainfall ranges from 800 mm to 1,000 mm, which, combined with steep terrain, increases the risk of landslides.

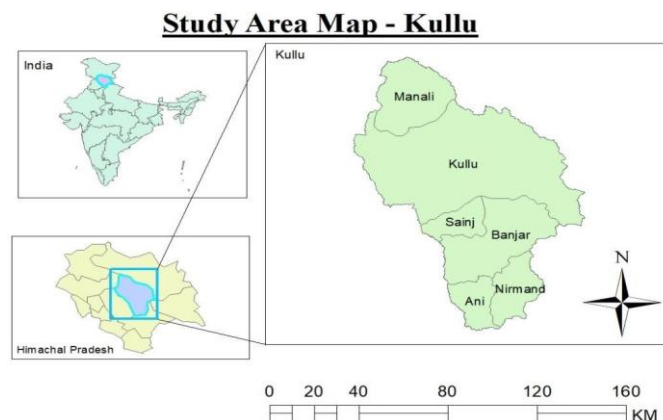


Figure 5.1: STUDY AREA MAP

CHAPTER 6

LANDSLIDE INVENTORY MAP

This landslide inventory map provides a spatial record of past landslide occurrences in the Kullu district. Historical landslide data was acquired in the form of polygon shapefiles from the Bhukosh by the Government of India, which is designated as one of the nodal agencies responsible for collecting past landslide incidence data in India.

A total of 399 landslide locations were obtained for the region. This landslide inventory data is critical for developing landslide susceptibility models, serving as a foundation for training and validating machine learning algorithms. By correlating the historical landslide locations with topographical, geological, and environmental variables, the inventory provides a basis for identifying landslide-prone areas.

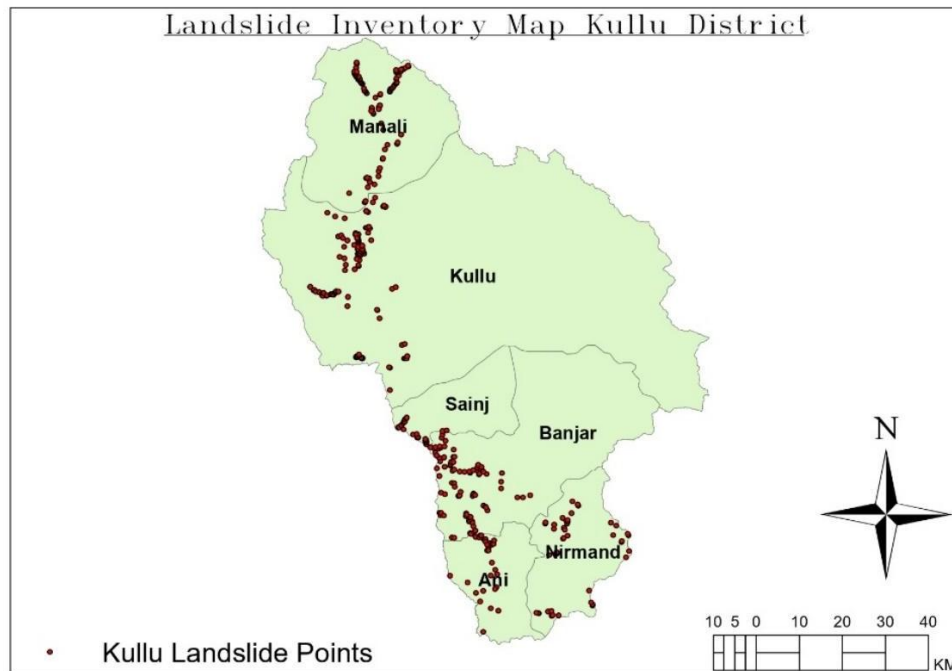


Figure 6.1: LANDSLIDE INVENTORY MAP

CHAPTER 7

LANDSLIDE CONDITIONING FACTORS

7.1 SLOPE

Known to depict the inclination of prevailing slopes in an area, the slope map was derived from the DEM in degrees using the spatial analyst surface tool of the GIS software and is said to have an impact on surface runoff and contribute to slope instability. The resulting map was then categorized into five classes, namely; 0° – 15° , 16° – 25° , 26° – 35° , 36° – 45° and $>45^{\circ}$.

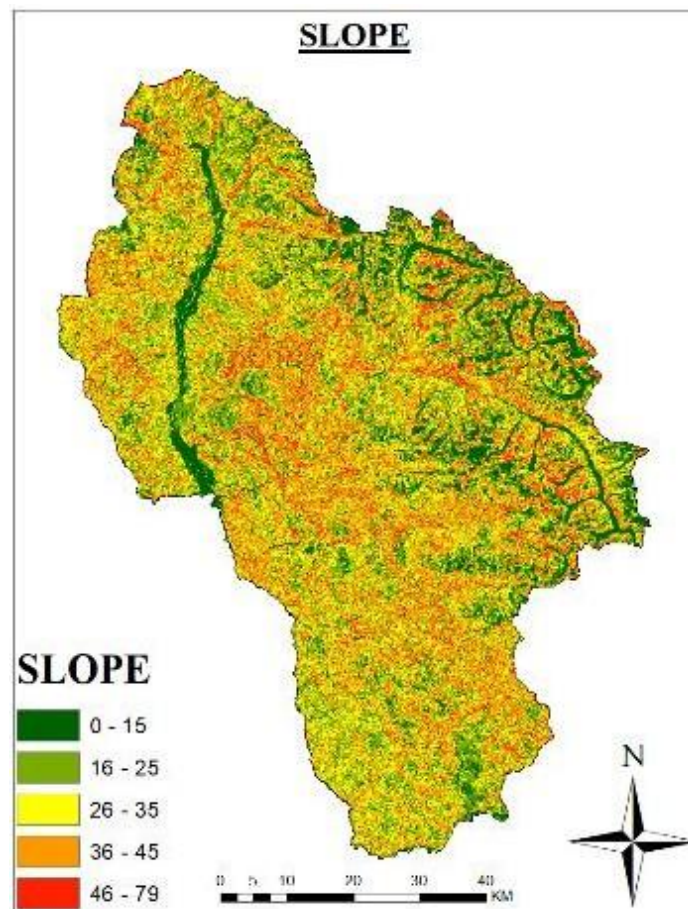


Figure 7.1: SLOPE

7.2 ASPECT

The aspect factor, which describes the spatial distribution of each topographical direction, is critical in determining slope stability. Furthermore, the curvature factor reflects topographical morphology. The aspect map was calculated from the DEM in ArcGIS 10.7 software. The aspect map was divided into five groups.

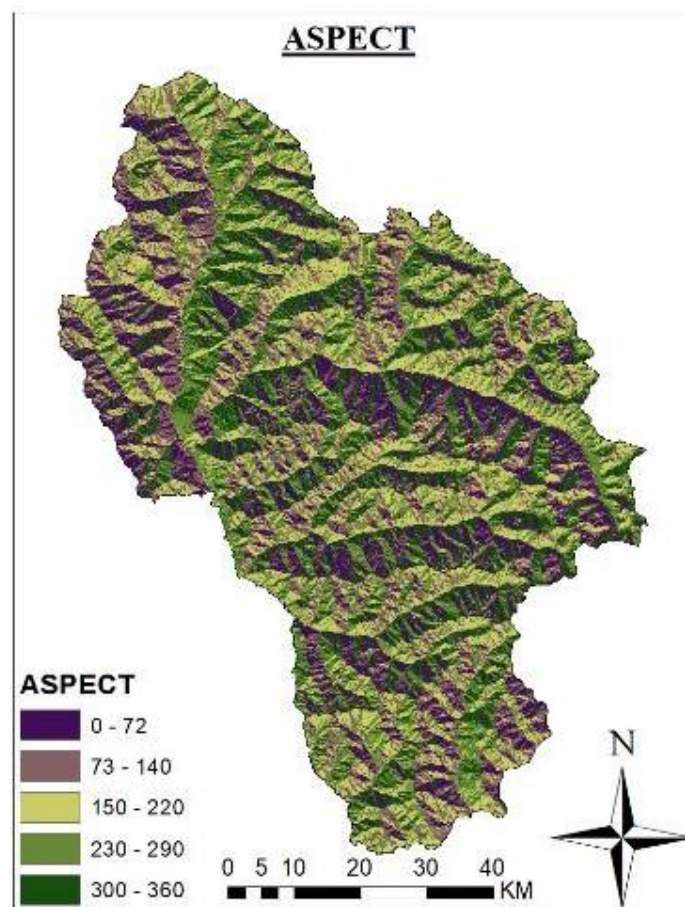


Figure7.2: ASPECT

7.3 DISTANCE FROM STREAM

Drainage does play an important role in slope instability, due to the action of under-cutting and increase in slope saturation. Also, bank erosion caused by high stream discharge velocity as well as toe erosion have a consequential impact on the area's landslide activity which is further enhanced by heavy rainfall.

The hydrology tools of the GIS platform were used to delineate the river networks, more specifically, by using the stream order tool. The Euclidean distance tool was then employed to create a buffer distance of 100 m intervals from the generated stream network. Five distinct classes resulted namely, 500 m, 1000 m, 1500 m, 2000 m and >2000m.

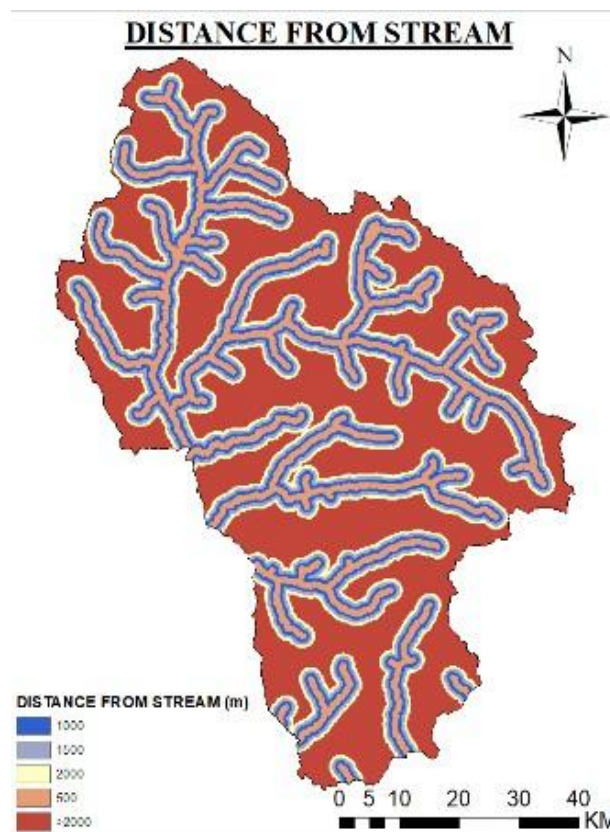


Figure7.3 : DISTANCE FROM STREAM

7.4 CURVATURE

Curvature, a key factor influencing slope stability, was classified into five categories: **Highly Concave** (high water accumulation and susceptibility), **Moderately Concave** (moderate susceptibility), **Flat** (neutral influence), **Moderately Convex** (low susceptibility), and **Highly Convex** (minimal susceptibility). These classes were derived using curvature analysis in ArcGIS to support the study of landslide susceptibility.

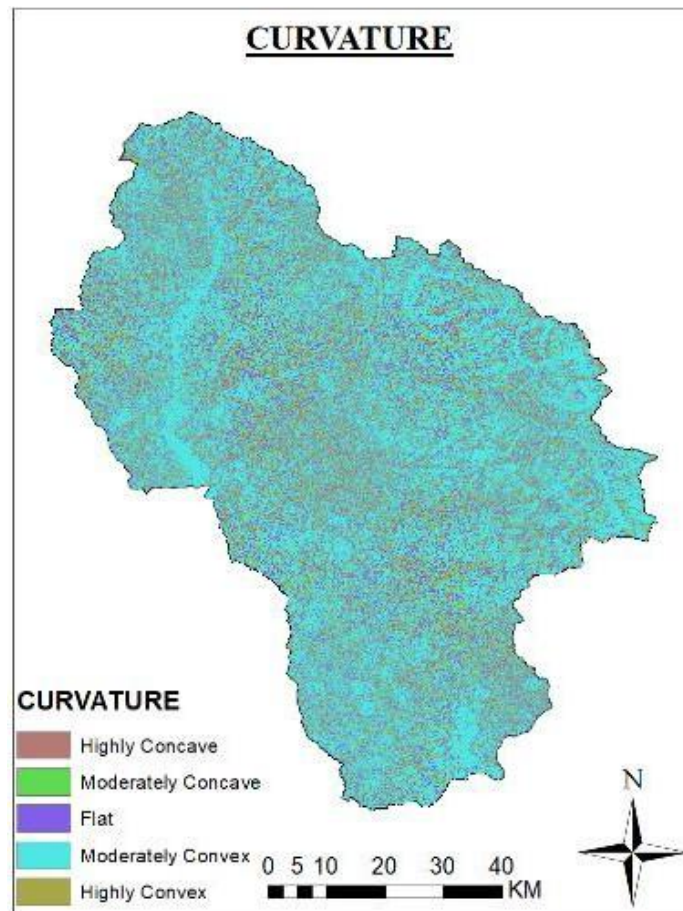


Figure 7.4: CURVATURE

7.5 ELEVATION

Elevation plays a significant role in influencing slope stability and landslide susceptibility. For this study, the elevation was classified into six categories: **<1500 m**, **1500–2500 m**, **2500–3500 m**, **3500–4500 m**, **4500–5500 m**, and **>5500 m**. These classes were created using GIS tools to reflect the varying topographical features of the region. Lower elevations (<1500 m) are more prone to human intervention and development, increasing landslide susceptibility, while higher elevations (>5500 m) generally exhibit reduced susceptibility due to limited accessibility and less anthropogenic activity.

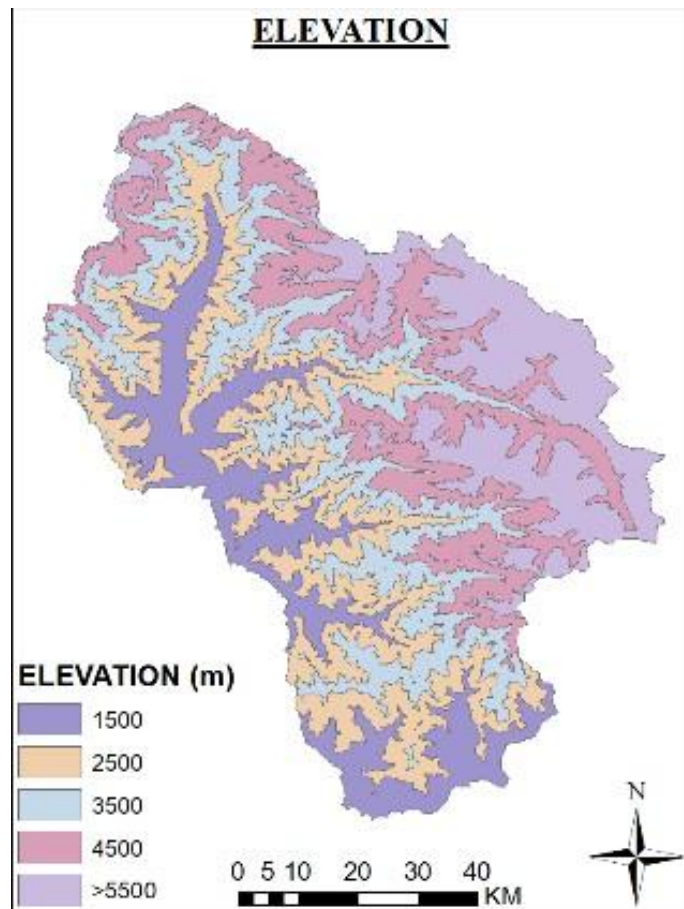


Figure 7.5 :ELEVATION

7.6 LITHOLOGY

The lithology shapefile, acquired from the USGS, contained four lithological units, each having distinct structure, strength, plasticity potential, and composition. The influence of each of these lithostratigraphic units on slope instability was therefore evaluated for deeper insight into their relationship to previous landslide occurrences. The lithology map was finally prepared after a process of extraction, rasterization, and resampling into 10 m cell resolution.

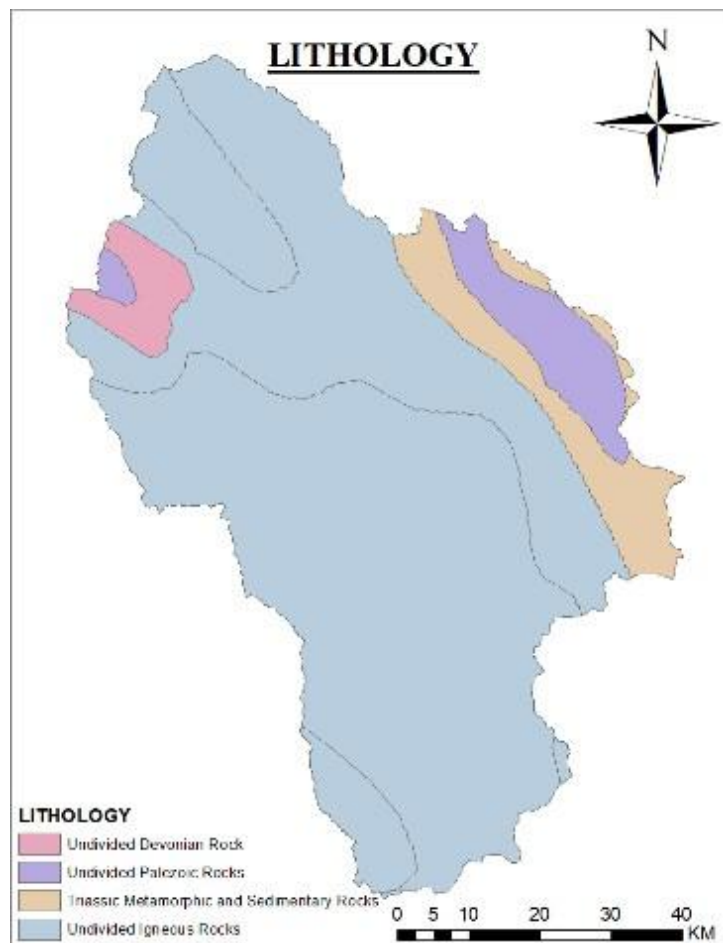


Figure 7.6: LITHOLOGY

7.7 HILLSHADE

Hillshade, an important parameter for terrain analysis, was classified into five categories based on illumination intensity: **Low Illumination**, **Moderate Low Illumination**, **Moderate Illumination**, **High Illumination**, and **Very High Illumination**.

These classes represent variations in sunlight exposure, with low illumination corresponding to shadowed, north-facing slopes that retain more moisture and may be more prone to instability, while high illumination areas are typically well-exposed, drier, and more stable. The classification aids in providing critical insights for topographical and geomorphological studies.

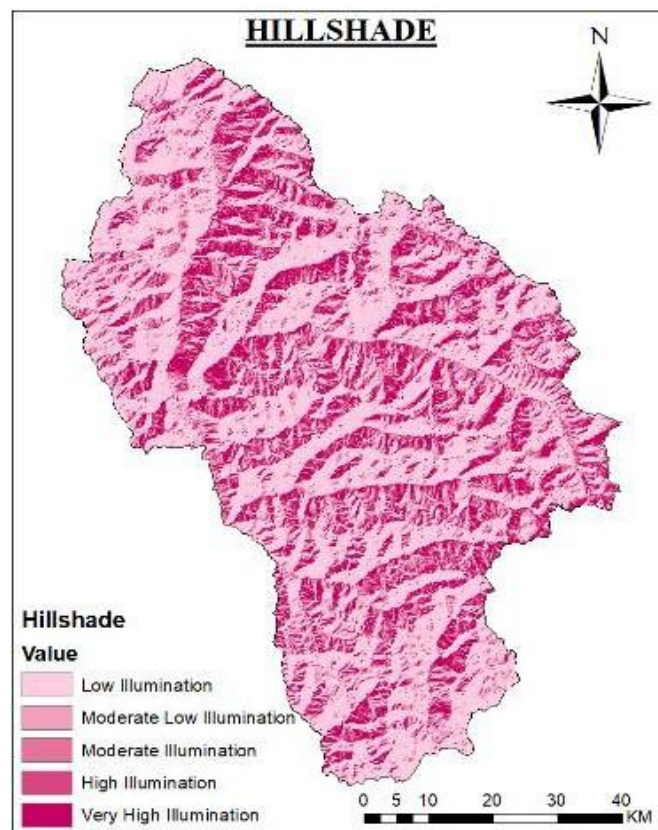


Figure 7.7: HILLSHADE

7.8 CONTOUR

Contours, essential for understanding topographical variation, were classified into five elevation categories: **800.00–1600.00 m**, **1600.01–2800.00 m**, **2800.01–4000.00 m**, **4000.01–4800.00 m**, and **4800.01–6400.00 m**. These categories represent altitudinal differences, with lower elevations often associated with river valleys, agricultural activities, and human settlements, while higher elevations correspond to rugged terrain, alpine ecosystems, and potential snow-covered regions.

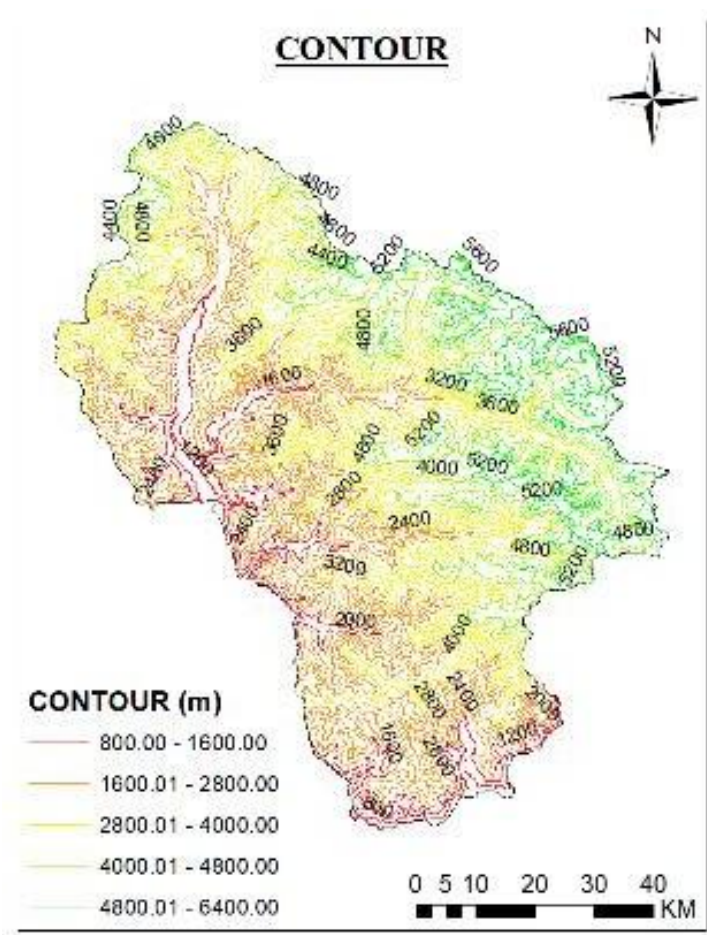


Figure7.8 : CONTOUR

7.9 TOPOGRAPHIC WETNESS INDEX (TWI)

The Topographic Wetness Index (TWI) is a crucial factor in assessing slope stability, as it measures the potential for water accumulation in a given area. TWI is influenced by both the local slope and upstream contributing areas, representing the tendency of soil to become saturated. Higher TWI values indicate areas where water is likely to accumulate, which in turn increases the potential for landslides due to reduced soil strength.

A classification scheme was applied in the GIS platform, creating several TWI categories that represent different levels of soil moisture saturation. These categories help in understanding the variation of landslide susceptibility across the region.

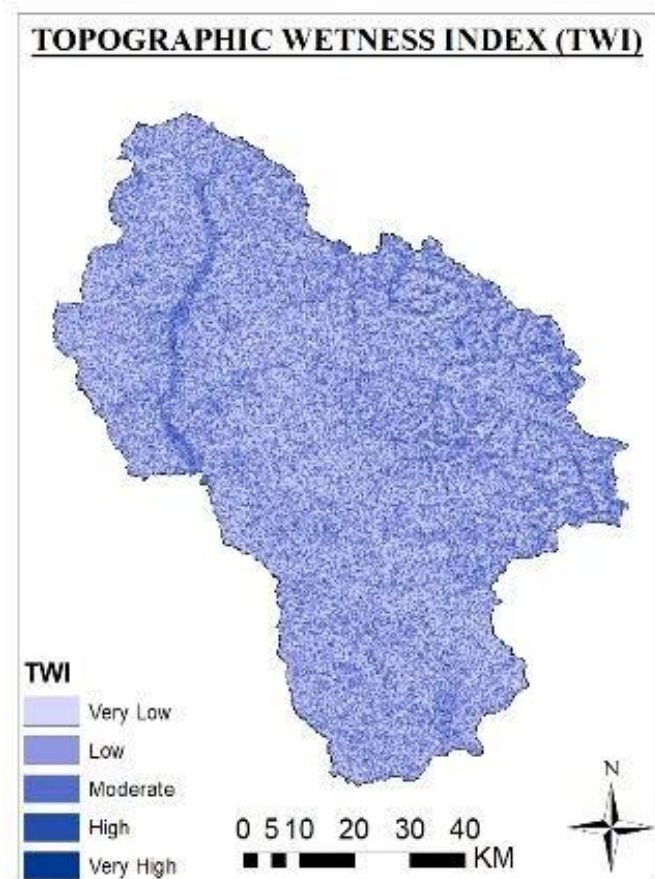


Figure 7.9: TWI

7.10 ROUGHNESS

Roughness is a critical topographic factor that influences the stability of slopes and the occurrence of landslides. It measures the irregularity and variability of the terrain surface, with higher roughness values indicating more rugged and uneven terrain. In mountainous regions like Kullu, roughness plays a significant role in determining how rainfall, vegetation, and soil interact with the slope surface.

For this study, roughness was calculated using Digital Elevation Model (DEM) data within a GIS platform. Areas with higher terrain roughness tend to experience more slope instability due to the uneven distribution of surface water runoff and soil mass movement.

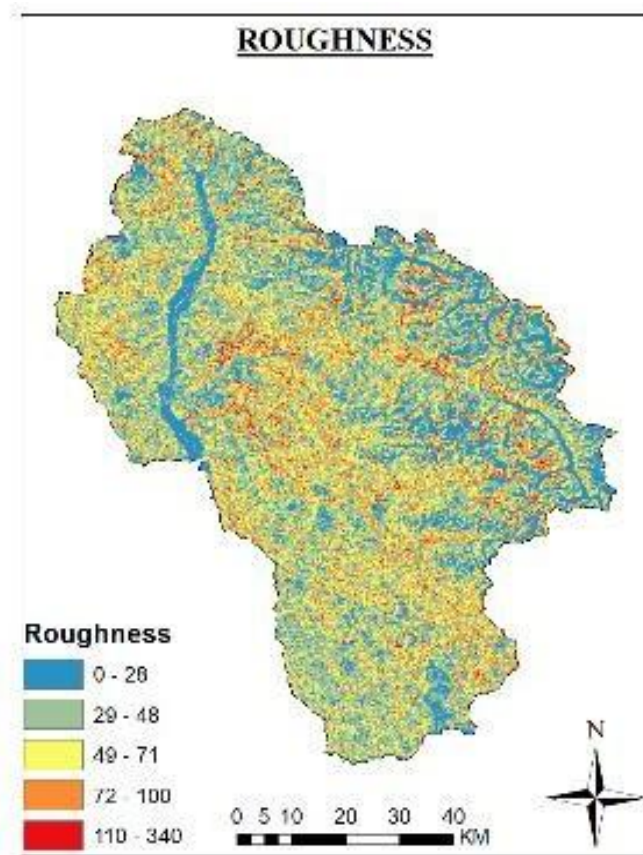


Figure 7.10: ROUGHNESS

CHAPTER 8

EMPIRICAL TECHNIQUE

8.1 Introduction

Frequency Ratio is an empirical technique used to assess the relationship between landslide occurrences and conditioning factors.

It calculates the likelihood of landslide occurrence based on the distribution of each factor class.

8.2 Formula

$$FR = (\text{Landslide Pixels in Factor Class} / \text{Total Landslide Pixels}) \div (\text{Total Pixels in Factor Class} / \text{Total Pixels in Study Area})$$

The resulting ratio represents the correlation strength between the factor class and landslide occurrence.

$$FR = \left(\frac{P_L}{\sum_{i=1}^n P_L} \right) / \left(\frac{P_C}{\sum_{i=1}^n P_C} \right) \quad (8.1)$$

where P_L = Landslide pixels contained in a factor class, P_C = Pixels of a factor class.

Categorize landslide conditioning factors (e.g., slope, aspect, elevation) into classes. Calculate the FR value for each class of the conditioning factors. Assign weights to the classes based on FR values.

8.3 Outcome

Generates weighted maps for each conditioning factor. Helps in creating a combined **landslide susceptibility map** by summing up weighted factors.

8.4 Application

Due to its data-driven approach, the Frequency Ratio (FR) method is widely used in landslide susceptibility mapping. It evaluates the relationship between past landslide occurrences and Landslide Conditioning Factors (LCFs) by calculating the probability of landslide presence within different factor classes. This method helps quantify each factor's contribution and assigns weights accordingly.

FR is commonly applied in geospatial analysis using GIS tools to generate landslide susceptibility maps. The method enables accurate zoning of landslide-prone areas by integrating historical landslide data with environmental and topographical parameters. These susceptibility maps assist in disaster preparedness, infrastructure planning, and risk assessment, helping policymakers make informed decisions for mitigation strategies.

8.5 Advantages of Frequency Ratio

One of the key advantages of the Frequency Ratio method is its simplicity and efficiency in analyzing landslide susceptibility. Since it is based on historical data, it provides objective and quantifiable results without relying on subjective expert opinions. Additionally, it is easy to implement using GIS software, making it a preferred choice for regional-scale susceptibility assessments.

Another significant advantage is its flexibility, which can be applied to various terrains and environmental conditions. The method also allows for comparative analysis with other models, helping researchers and planners evaluate the effectiveness of different susceptibility assessment techniques. Furthermore, the statistical nature of FR improves accuracy, ensuring reliable hazard predictions in landslide-prone regions.

TABLE 8.1: FREQUENCY RATIO CALCULATION

Parameter	Classes	Class Pixels	% Class Pixels	Landslide Pixels	% Landslide Pixels	FR	RF	RF (non%)	RF (INT)	Min RF	Max RF	Max-Min RF	(Max-Min) Min RF	PR
Slope	1	647 471	9.5 68	3680.6 39941	11.26 1	1.1 769	0.16 959	16.9 593	16					
	2	964 952	14. 260	5663.5 19909	17.32 8	1.2 151	0.17 510	17.5 100	17					
	3	130 195 1	19. 240	6894.7 1989	21.09 4	1.0 964	0.15 799	15.7 989	15					
	4	141 720 3	20. 944	6803.9 99891	20.81 7	0.9 939	0.14 323	14.3 231	14					
	5	125 203 0	18. 503	4821.1 19923	14.75 0	0.7 972	0.11 488	11.4 879	11					
	6	839 960	12. 413	3499.1 99944	10.70 6	0.8 625	0.12 428	12.4 284	12					
	7	343 165	5.0 71	1321.9 19979	4.044	0.7 975	0.11 492	11.4 923	11					
		676 673 2		32685. 12		6.9 394				0.11488	0.17 510	0.06 022	0.00 692	8. 70
Distance From Stream	1	889 849	13. 124	14359. 67977	43.91 6	3.3 461	0.55 315	55.3 149	55					
	2	837 689	12. 355	3784.3 19939	11.57 4	0.9 367	0.15 485	15.4 853	15					
	3	815 942	12. 034	2838.2 39955	8.680	0.7 213	0.11 923	11.9 235	11					
	4	798 463	11. 777	1697.7 59973	5.192	0.4 409	0.07 288	7.28 84	7					
	5	343 813 4	50. 709	10018. 07984	30.63 8	0.6 042	0.09 988	9.98 79	9					

		678 007 7		32698. 08		6.0 492				0.09988	0.55 315	0.45 327	0.04 527	10 .0 1
Topog raphic Wetne ss Index	1	236 612 0	34. 967	9447.8 39849	28.91 7	0.8 27	0.11 921	11.9 213	11					
	2	259 402 2	38. 335	13504. 31978	41.33 3	1.0 78	0.15 543	15.5 427	15					
	3	128 405 1	18. 976	6324.4 79899	19.35 7	1.0 20	0.14 705	14.7 052	14					
	4	426 583	6.3 04	1982.8 79968	6.069	0.9 63	0.13 878	13.8 778	13					
	5	959 56	1.4 18	1412.6 39977	4.324	3.0 49	0.43 953	43.9 529	43					
		676 673 2		32672. 15948		6.9 37				0.11921	0.43 953	0.32 032	0.03 819	8. 39
Rough ness	1	129 699 6	19. 129	6985.4 39888	21.37 2	1.1 17	0.21 087	21.0 866	21					
	2	209 544 0	30. 906	12000. 95981	36.71 7	1.1 88	0.22 423	22.4 230	22					
	3	176 416 1	26. 020	7270.5 59884	22.24 4	0.8 55	0.16 135	16.1 355	16					
	4	107 508 9	15. 856	4250.8 79932	13.00 6	0.8 20	0.15 481	15.4 806	15					
	5	447 110	6.5 94	1982.8 79968	6.067	0.9 20	0.17 363	17.3 634	17					
	6	101 333	1.4 95	194.39 99969	0.595	0.3 98	0.07 511	7.51 10	7					
		678 012 9		32685. 12		5.2 98				0.07511	0.22 423	0.14 912	0.01 120	13 .3 1

Hillshade	1	386 190 5	57. 119	19090. 08	58.38 3	1.0 22	0.20 729	20.7 292	20					
	2	456 610	6.7 53	1516.3 2	4.637	0.6 87	0.13 926	13.9 259	13					
	4	500 197	7.3 98	2643.8 4	8.086	1.0 93	0.22 165	22.1 652	22					
	6	607 601	8.9 87	3589.9 2	10.97 9	1.2 22	0.24 777	24.7 767	24					
	7	133 484 9	19. 743	5857.9 2	17.91 5	0.9 07	0.18 403	18.4 030	18					
		676 116 2		32698. 08		4.9 31				0.13926	0.24 777	0.10 851	0.01 511	7. 18
Elevation	1	106 375	1.5 69	194.40	0.595	0.3 79	0.02 995	2.99 51	2					
	2	223 904	3.3 02	2462.4 0	7.531	2.2 80	0.18 024	18.0 238	18					
	3	206 797	3.0 50	4250.8 8	13.00 0	4.2 62	0.33 689	33.6 887	33					
	4	345 180	5.0 91	4626.7 2	14.15 0	2.7 79	0.21 967	21.9 673	21					
	5	125 623 0	18. 528	4911.8 4	15.02 2	0.8 11	0.06 408	6.40 80	6					
	6	130 200 7	19. 203	3499.2 0	10.70 2	0.5 57	0.04 405	4.40 46	4					
	7	166 765 1	24. 596	4821.1 2	14.74 4	0.5 99	0.04 738	4.73 80	4					
	8	167 198 5	24. 660	7931.5 2	24.25 7	0.9 84	0.07 775	7.77 45	7					
		678 012 9		32698. 08		12. 652				0.02995	0.33 689	0.30 694	0.00 919	33 .3 9

Aspect	1	698 080	10. 316	2838.2 4	8.680	0.8 41	0.09 307	9.30 69	9					
	2	655 031	9.6 80	3123.3 6	9.552	0.9 87	0.10 915	10.9 149	10					
	3	619 183	9.1 50	3019.6 8	9.235	1.0 09	0.11 164	11.1 635	11					
	4	786 613	11. 625	4250.8 8	13.00 0	1.1 18	0.12 370	12.3 702	12					
	5	857 871	12. 678	4160.1 6	12.72 3	1.0 04	0.11 101	11.1 006	11					
	6	881 251	13. 023	4341.6 0	13.27 8	1.0 20	0.11 277	11.2 774	11					
	7	737 241	10. 895	4445.2 8	13.59 5	1.2 48	0.13 802	13.8 022	13					
	8	716 266	10. 585	4536.0 0	13.87 2	1.3 11	0.14 496	14.4 963	14					
	9	815 196	12. 047	1982.8 8	6.064	0.5 03	0.05 568	5.56 79	5					
		676 673 2		32698. 08		9.0 41				0.05568	0.14 496	0.08 928	0.00 497	17 .9 6
Curva ture	1	150 106 1	22. 139	7374.2 4	22.55 3	1.0 19	0.34 935	34.9 348	34					
	2	379 029 3	55. 903	19271. 52	58.93 8	1.0 54	0.36 156	36.1 562	36					
	3	148 877 5	21. 958	6052.3 2	18.51 0	0.8 43	0.28 909	28.9 090	28					
		678 012 9		32698. 08		2.9 16				0.28909	0.36 156	0.07 247	0.02 095	3. 46
Conto ur	1	386 190 5	57. 119	19090. 08	58.38 29	1.0 22	0.20 729	20.7 292	20					
	2	456 610	6.7 53	1516.3 2	4.637 3	0.6 87	0.13 926	13.9 259	13					

	3	500 197	7.3 98	2643.8 4	8.085 6	1.0 93	0.22 165	22.1 652	22					
	4	607 601	8.9 87	3589.9 2	10.97 90	1.2 22	0.24 777	24.7 767	24					
	5	133 484 9	19. 743	5857.9 2	17.91 52	0.9 07	0.18 403	18.4 030	18					
		676 116 2		32698. 08		4.9 31				0.13926	0.24 777	0.10 851	0.01 511	7. 18
Lithol ogy	0	187 381 5	27. 637	10018. 08	30.63 81	1.1 09	0.21 531	21.5 312	21					
	1	502 077	7.4 05	0.00	0.000 0	0.0 00	0.00 000	0.00 00	0					
	2	408 960	6.0 32	2734.5 6	8.363 1	1.3 86	0.26 929	26.9 289	26					
	3	631	0.0 09	0.00	0.000 0	0.0 00	0.00 000	0.00 00	0					
	4	358 169	5.2 83	0.00	0.000 0	0.0 00	0.00 000	0.00 00	0					
	5	319 849 9	47. 175	18519. 84	56.63 89	1.2 01	0.23 319	23.3 186	23					
	6	196 269	2.8 95	194.40	0.594 5	0.2 05	0.03 989	3.98 89	3					
	7	370 35	0.5 46	0.00	0.000 0	0.0 00	0.00 000	0.00 00	0					
	8	204 618	3.0 18	1231.2 0	3.765 4	1.2 48	0.24 232	24.2 324	24					
		678 007 3		32698. 08		5.1 49				0.03988 924995	0.26 929	0.22 940	0.00 915	25 .0 7

CHAPTER 9

STATISTICAL TECHNIQUE

9.1 Introduction

Shannon Entropy is a statistical approach used in landslide susceptibility mapping to measure the uncertainty in data distribution. It helps determine the significance of Landslide Conditioning Factors (LCFs) by analyzing their probability and contribution to landslide occurrences. Factors with higher entropy values indicate more randomness, while those with lower entropy strongly influence landslide susceptibility.

This method assigns weights to each LCF by calculating entropy and information gain, ensuring an objective and data-driven assessment. The weighted factors are then combined to generate a landslide susceptibility map, improving the accuracy of hazard prediction and reducing biases in factor selection.

9.2 Formula

$$P_{ij} = \% \text{ landslide pixels} / \% \text{ class pix} \quad (9.1)$$

Where P_{ij} from Eq. (9.1) represents the frequency ratio values, and (P_{ij}) from Eq. (9.2) gives the probability density value of each class.

$$(P_{ij}) = P_{ij} / \sum_{j=1}^{n_j} P_{ij} \quad (9.2)$$

H_j and H_{jmax} from Eqs. (3) and (4) denote the entropy values for each class, whereas n_j is the number of classes in each factor.

$$H_j = \sum_{i=1}^{n_j} (P_{ij}) \log_2(P_{ij}) \quad (9.3)$$

$$H_{jmax} = \log_2(n_j) \quad (9.4)$$

The information coefficient, I_{ij} , and the final weight index, W_j , were evaluated using

Eqs. (5) and (6), respectively.

$$I_{ij} = (H_{j\max} - H_j) / H_{j\max} \quad (9.5)$$

$$W_j = I_{ij} \times P_j \quad (9.6)$$

9.3 Outcome of Shannon Entropy

The Shannon Entropy method provides a quantitative and objective landslide susceptibility assessment by measuring the uncertainty and significance of Landslide Conditioning Factors (LCFs). By analyzing the probability distribution of landslide occurrences, it assigns weights based on information gain, ensuring an accurate and data-driven susceptibility map.

The final landslide susceptibility map categorizes the study area into different risk zones, helping identify regions with high landslide potential. This approach enhances predictive accuracy, reduces bias in factor selection, and supports effective disaster management, risk assessment, and land-use planning.

9.4 Application in Landslide Susceptibility Mapping

Shannon Entropy plays a crucial role in landslide susceptibility mapping by evaluating the importance of each Landslide Conditioning Factor (LCF). By analyzing the probability distribution of landslide occurrences, it helps in assigning appropriate weights to different factors based on their contribution to landslide susceptibility.

This ensures a more data-driven and objective approach, leading to more accurate susceptibility predictions and improved hazard assessment.

9.5 Advantages

One of the main advantages of Shannon Entropy is its objective approach to factor weighting, which reduces subjective biases in susceptibility assessment. It also considers

the information content of each factor, ensuring that influential factors are appropriately weighted.

Additionally, this method can be integrated with other statistical and machine learning techniques, further enhancing the accuracy and reliability of landslide susceptibility

TABLE 9.1: SHANNON ENTROPY CALCULATION

Parameter	Classes	Class Pixels	% Class Pixels	Landslide Pixels	% Landslide Pixels	FR	Shannon Entropy			
							Pij	Ej	1-Ej	Wj (Percentage)
Slope	1	647471	9.568	3680.64	11.261	1.1769	0.1696	-0.1307	0.161	0.054
	2	964952	14.260	5663.52	17.328	1.2151	0.1751	-0.1325		
	3	1301951	19.240	6894.72	21.094	1.0964	0.1580	-0.1266		
	4	1417203	20.944	6804.00	20.817	0.9939	0.1432	-0.1209		
	5	1252030	18.503	4821.12	14.750	0.7972	0.1149	-0.1080		
	6	839960	12.413	3499.20	10.706	0.8625	0.1243	-0.1125		
	7	343165	5.071	1321.92	4.044	0.7975	0.1149	-0.1080		
Total		6766732		32685.12		6.9394		-0.8392		
Distance From Stream	1	889849	13.124	14359.68	43.916	3.3461	0.5531	-0.1422	0.439	0.147
	2	837689	12.355	3784.32	11.574	0.9367	0.1549	-0.1254		
	3	815942	12.034	2838.24	8.680	0.7213	0.1192	-0.1101		

	4	79846 3	11.7 77	1697.76	5.192	0.44 09	0.07 29	- 0.08 29		
	5	34381 34	50.7 09	10018.0 8	30.638	0.60 42	0.09 99	- 0.09 99		
Total		67800 77		32698.0 8		6.04 92		- 0.56 06		
Topographic Wetness Index	1	23661 20	34.9 67	9447.84	28.917	0.82 7	0.11 92	- 0.11 01	0.36 6	0.122
	2	25940 22	38.3 35	13504.3 2	41.333	1.07 8	0.15 54	- 0.12 57		
	3	12840 51	18.9 76	6324.48	19.357	1.02 0	0.14 71	- 0.12 24		
	4	42658 3	6.30 4	1982.88	6.069	0.96 3	0.13 88	- 0.11 90		
	5	95956	1.41 8	1412.64	4.324	3.04 9	0.43 95	- 0.15 69		
Total		67667 32		32672.1 6		6.93 7		- 0.63 41		
Roughness	1	12969 96	19.1 29	6985.44	21.372	1.11 7	0.21 09	- 0.14 25	0.24 2	0.081
	2	20954 40	30.9 06	12000.9 6	36.717	1.18 8	0.22 42	- 0.14 56		
	3	17641 61	26.0 20	7270.56	22.244	0.85 5	0.16 14	- 0.12 78		
	4	10750 89	15.8 56	4250.88	13.006	0.82 0	0.15 48	- 0.12 54		

	5	447110	6.594	1982.88	6.067	0.920	0.1736	-0.1320		
	6	101333	1.495	194.40	0.595	0.398	0.0751	-0.0844		
Total		6780129		32685.12		5.298		-0.7579		
Hillshade	1	3861905	57.119	19090.08	58.383	1.022	0.2073	-0.1417	0.309	0.103
	2	456610	6.753	1516.32	4.637	0.687	0.1393	-0.1192		
	4	500197	7.398	2643.84	8.086	1.093	0.2217	-0.1450		
	6	607601	8.987	3589.92	10.979	1.222	0.2478	-0.1501		
	7	1334849	19.743	5857.92	17.915	0.907	0.1840	-0.1353		
Total		6761162		32698.08		4.931		-0.6913		
Elevation	1	106375	1.569	194.40	0.595	0.379	0.0300	-0.0456	0.231	0.077
	2	223904	3.302	2462.40	7.531	2.280	0.1802	-0.1341		
	3	206797	3.050	4250.88	13.000	4.262	0.3369	-0.1592		
	4	345180	5.091	4626.72	14.150	2.779	0.2197	-0.1446		

	5	12562 30	18.5 28	4911.84	15.022	0.81 1	0.06 41	- 0.07 65		
	6	13020 07	19.2 03	3499.20	10.702	0.55 7	0.04 40	- 0.05 97		
	7	16676 51	24.5 96	4821.12	14.744	0.59 9	0.04 74	- 0.06 28		
	8	16719 85	24.6 60	7931.52	24.257	0.98 4	0.07 77	- 0.08 62		
Total		67801 29		32698.0 8		12.6 52		- 0.76 87		
Aspect	1	69808 0	10.3 16	2838.24	8.680	0.84 1	0.09 31	- 0.09 60		
	2	65503 1	9.68 0	3123.36	9.552	0.98 7	0.10 91	- 0.10 50		
	3	61918 3	9.15 0	3019.68	9.235	1.00 9	0.11 16	- 0.10 63		
	4	78661 3	11.6 25	4250.88	13.000	1.11 8	0.12 37	- 0.11 23		
	5	85787 1	12.6 78	4160.16	12.723	1.00 4	0.11 10	- 0.10 60		
	6	88125 1	13.0 23	4341.60	13.278	1.02 0	0.11 28	- 0.10 69		
	7	73724 1	10.8 95	4445.28	13.595	1.24 8	0.13 80	- 0.11 87		
	8	71626 6	10.5 85	4536.00	13.872	1.31 1	0.14 50	- 0.12 16	0.05 75	0.019

	9	81519 6	12.0 47	1982.88	6.064	0.50 3	0.05 57	- 0.06 98		
Total		67667 32		32698.0 8		9.04 1		- 0.94 25		
Curvature	1	15010 61	22.1 39	7374.24	22.553	1.01 9	0.34 93	- 0.15 96	0.52 49	0.176
	2	37902 93	55.9 03	19271.5 2	58.938	1.05 4	0.36 16	- 0.15 97		
	3	14887 75	21.9 58	6052.32	18.510	0.84 3	0.28 91	- 0.15 58		
Total		67801 29		32698.0 8		2.91 6		- 0.47 51		
Contour	1	38619 05	57.1 19	19090.0 8	58.3829	1.02 2	0.20 73	- 0.14 17	0.30 87	0.103
	2	45661 0	6.75 3	1516.32	4.6373	0.68 7	0.13 93	- 0.11 92		
	3	50019 7	7.39 8	2643.84	8.0856	1.09 3	0.22 17	- 0.14 50		
	4	60760 1	8.98 7	3589.92	10.9790	1.22 2	0.24 78	- 0.15 01		
	5	13348 49	19.7 43	5857.92	17.9152	0.90 7	0.18 40	- 0.13 53		
Total		67611 62		32698.0 8		4.93 1		- 0.69 13		
Lithology	0	18738 15	27.6 37	10018.0 8	30.6381	1.10 9	0.21 53	- 0.14 36	0.35 05	0.117

	1	50207 7	7.40 5	0.00	0.0000	0.00 0	0.00 00	0.00 00		
	2	40896 0	6.03 2	2734.56	8.3631	1.38 6	0.26 93	- 0.15 34		
	3	631	0.00 9	0.00	0.0000	0.00 0	0.00 00	0.00 00		
	4	35816 9	5.28 3	0.00	0.0000	0.00 0	0.00 00	0.00 00		
	5	31984 99	47.1 75	18519.8 4	56.6389	1.20 1	0.23 32	- 0.14 74		
	6	19626 9	2.89 5	194.40	0.5945	0.20 5	0.03 99	- 0.05 58		
	7	37035	0.54 6	0.00	0.0000	0.00 0	0.00 00	0.00 00		
	8	20461 8	3.01 8	1231.20	3.7654	1.24 8	0.24 23	- 0.14 92		
Total		67800 73		32698.0 8		5.14 9		- 0.64 95		

CHAPTER 10

ANALYTICAL TECHNIQUE

10.1 Introduction

The Analytical Hierarchy Process (AHP) is a multi-criteria decision-making method used in landslide susceptibility mapping to assign relative weights to Landslide Conditioning Factors (LCFs). It is based on expert judgment and pairwise comparisons, ensuring a structured evaluation of factor importance.

AHP calculates weights through a comparison matrix, ranking factors based on their influence on landslides. A Consistency Ratio (CR) is used to validate the reliability of judgments. This method effectively incorporates expert knowledge but may introduce subjectivity compared to data-driven statistical approaches.

10.2 Formula

AHP calculates weights through pairwise comparisons, forming a judgment matrix. The weight (W) of each factor is determined using the eigenvector method:

$$AW = \lambda_{\max} W \quad (10.1)$$

Where:

A is the pairwise comparison matrix

W is the weight vector

λ_{\max} is the maximum eigenvalue

The Consistency Ratio (CR) ensures the reliability of judgments and is computed as follows:

$$CR = CI / RI \quad (10.2)$$

where:

$CI = (\lambda_{\max} - n) / (n - 1)$ (Consistency Index)

RI is the Random Index for a given matrix size

n is the number of factors

A CR value ≤ 0.1 indicates an acceptable level of consistency.

10.3 Outcome

The Analytical Hierarchy Process (AHP) generates a weighted landslide susceptibility map, categorizing areas into different risk zones based on factor importance. Incorporating expert judgment ensures a systematic prioritization of Landslide Conditioning Factors (LCFs), allowing for a more structured evaluation. This method aids in identifying high-risk areas, enabling authorities to implement effective landslide mitigation strategies and make informed decisions for disaster management.

10.4 Application

The Analytical Hierarchy Process (AHP) is widely used in landslide susceptibility mapping to assign relative importance to Landslide Conditioning Factors (LCFs). Using pairwise comparisons and expert judgment, AHP systematically ranks factors such as slope, elevation, lithology, and distance from streams based on their influence on landslides.

AHP is applied in geospatial analysis using GIS tools to generate weighted susceptibility maps. These maps help in risk assessment, infrastructure planning, and disaster mitigation by identifying high-risk zones. Additionally, AHP can be integrated with other statistical and machine learning models to enhance prediction accuracy and improve landslide hazard assessment in complex terrains.

10.5 Advantages

One of the key advantages of the Frequency Ratio method is its simplicity and efficiency in analyzing landslide susceptibility. Since it is based on historical data, it provides objective and quantifiable results without relying on subjective expert opinions.

Another major advantage is its flexibility, which can be applied to various terrains and environmental conditions. The method also allows for comparative analysis with other models, helping researchers and planners evaluate the effectiveness of different susceptibility assessment techniques.

TABLE 10.1 AHP MATRIX

Factors	Slope	Aspect	Curvature	Hillshade	Roughness	Contour	Elevation	TWI	Distance from Stream	Lithology
Slope	1	3	2	4	2	3	0.5	0.5	2	0.33
Aspect	0.33	1	0.5	2	0.5	1	0.33	0.33	0.5	0.25
Curvature	0.5	2	1	3	1	2	0.5	0.5	1	0.33
Hillshade	0.25	0.5	0.33	1	0.33	0.5	0.25	0.25	0.33	0.2
Roughness	0.5	2	1	3	1	2	0.5	0.5	1	0.33
Contour	0.33	1	0.5	2	0.5	1	0.33	0.33	0.5	0.25
Elevation	2	3	2	4	2	3	1	1	2	0.5
TWI	2	3	2	4	2	3	1	1	2	0.5
Distance from stream	0.5	2	1	3	1	2	0.5	0.5	1	0.33
Lithology	3	4	3	5	3	4	2	2	3	1
SUM	10.41	21.5	13.33	31	13.33	21.5	6.91	6.91	13.33	4.02

TABLE: 10.2 CI VALUES

Factors	Slope	Aspect	Curvature	Hillshade	Roughness	Contour	Elevation	TWI	Distance from stream	Lithology	Average	Lemda	CI	RCI	CR
Slope	0.10	0.14	0.15	0.13	0.15	0.14	0.07	0.07	0.15	0.08	0.12	10.21	0.024	1.49	0.016
Aspect	0.03	0.05	0.04	0.06	0.04	0.05	0.05	0.05	0.04	0.06	0.05	10.07	0.008	1.49	0.005
Curvature	0.05	0.09	0.08	0.10	0.08	0.09	0.07	0.07	0.08	0.08	0.08	10.10	0.011	1.49	0.007
Hillshade	0.02	0.02	0.02	0.03	0.02	0.02	0.04	0.04	0.02	0.05	0.03	10.11	0.013	1.49	0.009
Roughness	0.05	0.09	0.08	0.10	0.08	0.09	0.07	0.07	0.08	0.08	0.08	10.10	0.011	1.49	0.007
Contour	0.03	0.05	0.04	0.06	0.04	0.05	0.05	0.05	0.04	0.06	0.05	10.07	0.008	1.49	0.005
Elevation	0.19	0.14	0.15	0.13	0.15	0.14	0.14	0.14	0.15	0.12	0.15	10.31	0.035	1.49	0.023
TWI	0.19	0.14	0.15	0.13	0.15	0.14	0.14	0.14	0.15	0.12	0.15	10.31	0.035	1.49	0.023
Distance From Stream	0.05	0.09	0.08	0.10	0.08	0.09	0.07	0.07	0.08	0.08	0.08	10.10	0.011	1.49	0.007
Lithology	0.29	0.19	0.23	0.16	0.23	0.19	0.29	0.29	0.23	0.25	0.23	10.30	0.033	1.49	0.022

CHAPTER 11

RESULTS

11.1 DISCUSSION

Landslide Susceptibility Maps were generated using three different methods: Frequency Ratio (FR), Shannon Entropy (SE), and Analytical Hierarchy Process (AHP). These models help in identifying landslide-prone areas by analyzing environmental factors such as slope, elevation, aspect, and lithology.

Each technique applies a unique approach to weigh the contributing factors, resulting in different susceptibility classifications.

Frequency Ratio (FR): A data-driven empirical method that calculates landslide probability based on historical landslide occurrences within different factor classes.

Shannon Entropy (SE): A statistical method that measures the randomness of factor distribution and assigns weights based on information gain.

Analytical Hierarchy Process (AHP): A structured decision-making technique that uses expert judgment and pairwise comparisons to assign relative importance to conditioning factors.

The results of this study provide a comparative analysis of three landslide susceptibility mapping techniques: Frequency Ratio (FR), Shannon Entropy (SE), and Analytical Hierarchy Process (AHP). Each model was evaluated based on its predictive accuracy and ability to classify landslide-prone areas effectively. The Frequency Ratio model achieved the highest accuracy with an AUC value of 0.738, followed closely by the Shannon Entropy model (AUC = 0.735). Both models demonstrated strong predictive capabilities, highlighting the effectiveness of data-driven and statistical approaches. In contrast, the AHP model yielded a lower AUC value of 0.635, indicating limitations in factor weighting based on expert judgment.

Susceptibility Map Using AHP

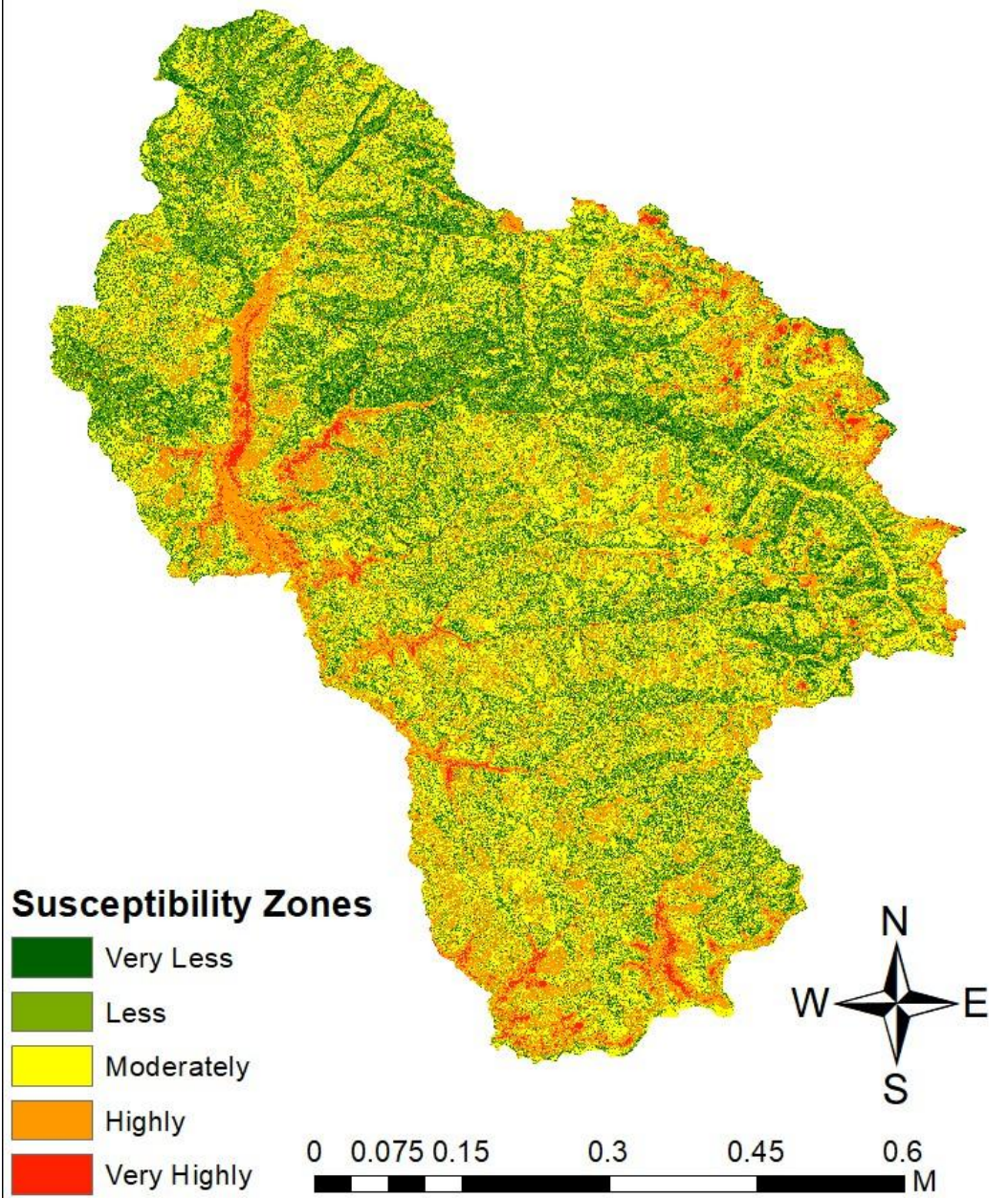


Figure 11.1 Susceptibility map using AHP

Susceptibility Map Using Frequency Ratio

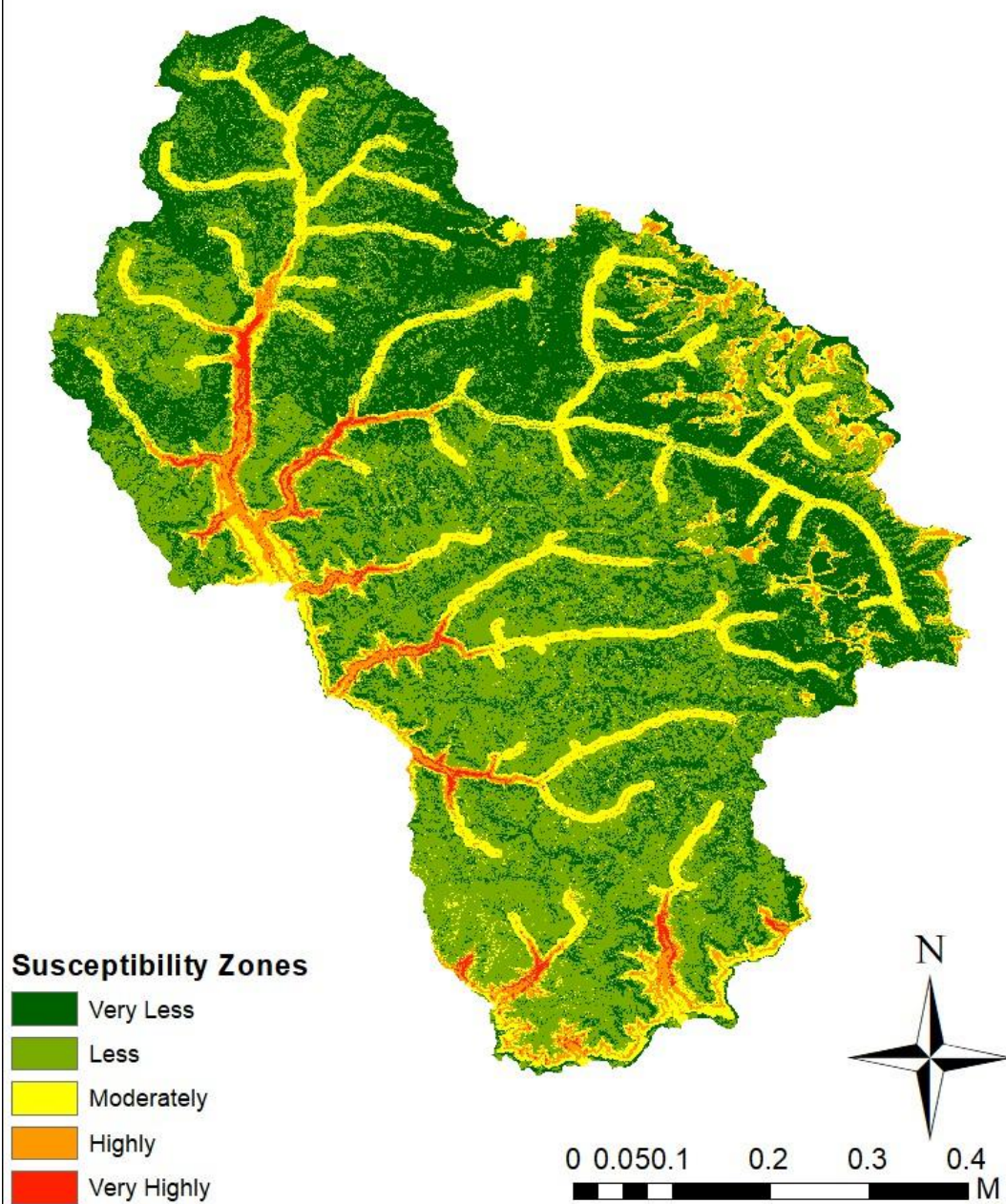


Figure 11.2 Susceptibility map using Frequency Ratio

Susceptibility Map Using Shannon Entropy

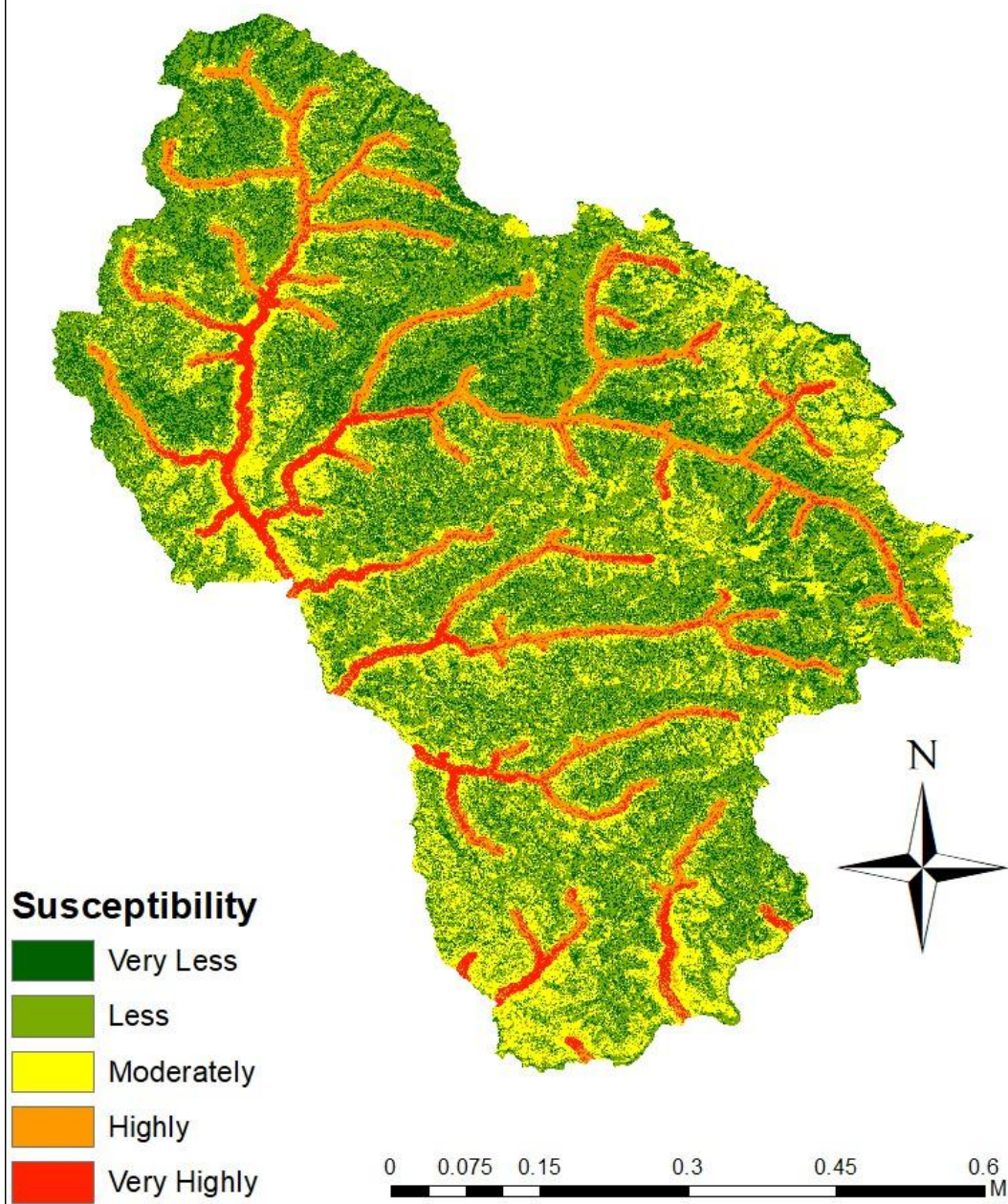


Figure 11.3 Susceptibility map using Shannon Entropy

11.2 VALIDATION

Validation is a crucial step in assessing the performance and reliability of a predictive model. It ensures that the model is effective on training data and performs well on unseen data. In landslide susceptibility mapping and other machine learning applications, validation helps in determining how accurately the model classifies areas as susceptible or non-susceptible. Various validation techniques, such as k-fold cross-validation, hold-out validation, and statistical metrics, are used to evaluate model effectiveness.

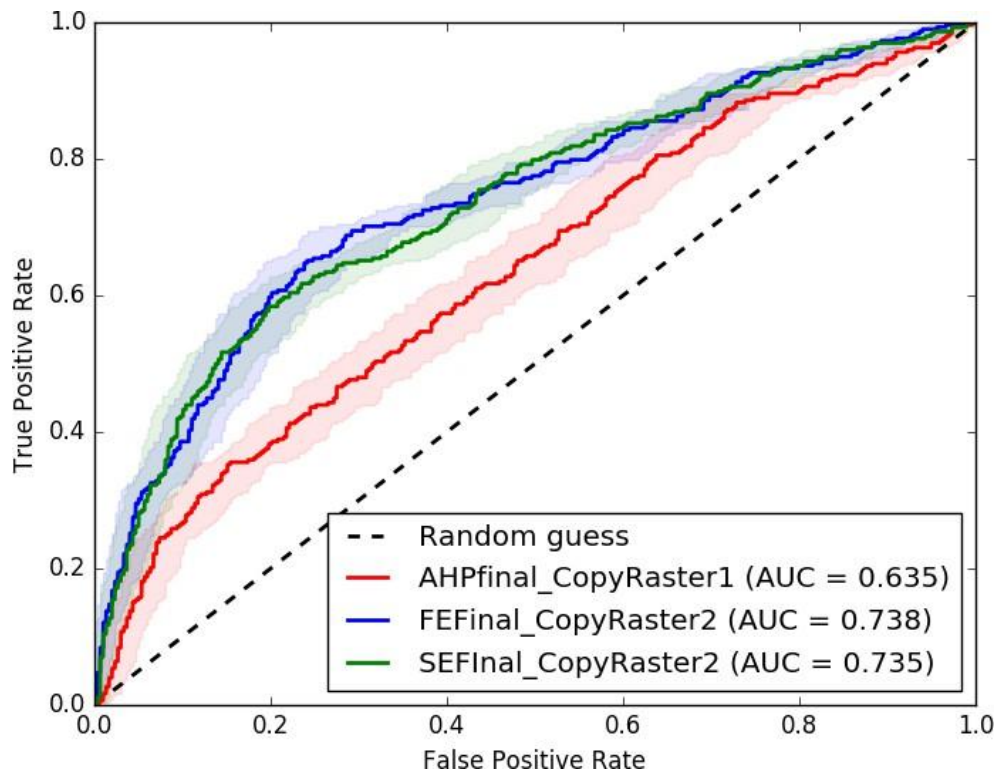


Figure 11.4 Success Rate Curve

One crucial measure of validation is the success rate curve, which assesses how well the model predicts landslide-prone areas based on the training dataset. It is generated by plotting the cumulative percentage of correctly predicted landslide areas against the total study area. A higher success rate indicates that the model effectively captures patterns in the training data and is well-calibrated for mapping susceptibility.

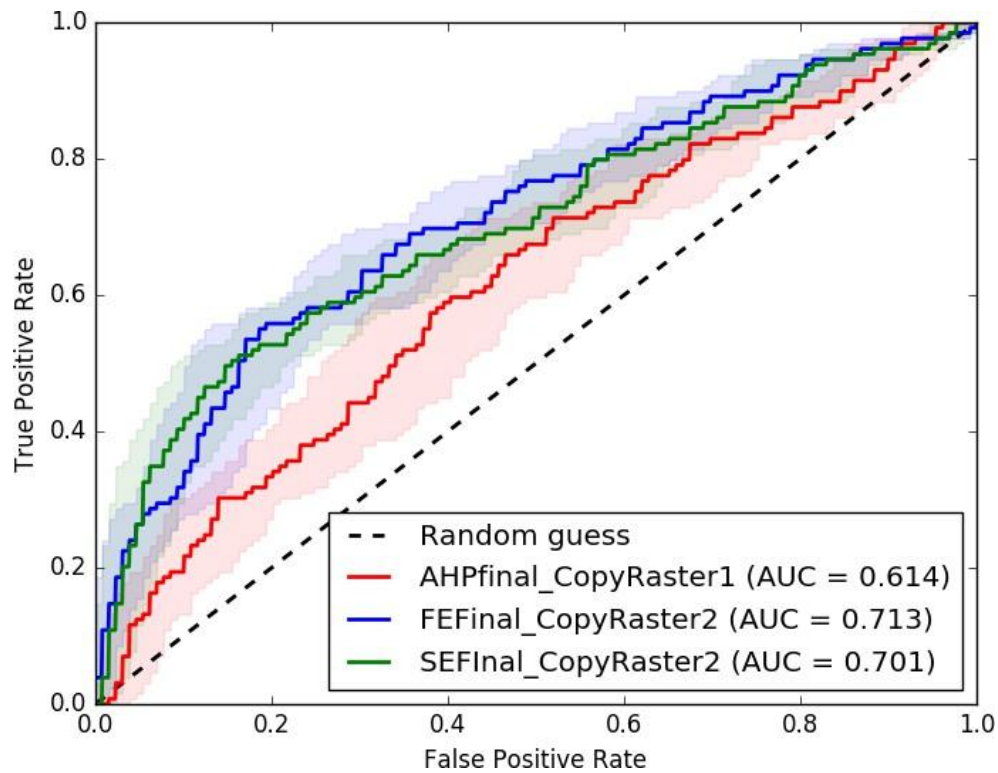


Figure 11.5 Prediction Rate Curve

Similarly, the prediction rate curve evaluates the model's ability to predict landslide occurrences on test data. It is derived from an independent dataset and helps determine how well the model generalizes beyond the training dataset. A model with a high prediction rate is considered robust and reliable for practical applications, as it indicates strong generalization capabilities.

In addition to these curves, true positives and negatives play a critical role in validation. True positives (TP) refer to areas correctly identified as landslide-prone, while true negatives (TN) indicate non-landslide areas correctly classified by the model. These values are crucial for calculating performance metrics such as accuracy, sensitivity, specificity, and the area under the curve (AUC). A well-validated model should have a high TP rate while maintaining a low false positive and false negative rate to ensure accurate susceptibility mapping.

CHAPTER 12

CONCLUSION AND FUTURE FOCUS

12.1 CONCLUSION

Landslide susceptibility mapping was conducted in the Kullu District of Himachal Pradesh using three techniques: Frequency Ratio (FR), Shannon Entropy (SE), and Analytical Hierarchy Process (AHP). The generated susceptibility maps were validated using Area Under the Curve (AUC) values, where the FR model achieved the highest predictive accuracy ($AUC = 0.738$), followed closely by the SE model ($AUC = 0.735$), indicating their strong predictive capabilities. In contrast, the AHP model exhibited lower accuracy ($AUC = 0.635$), suggesting limitations in factor weighting through expert judgment. To further evaluate model performance, Success Rate and Prediction Rate curves were developed, helping to assess both the model fit with training data and its predictive capability with testing data.

The results highlight that statistical-based models (FR and SE) outperform AHP in predicting landslide-prone areas, making them more reliable for hazard assessment. The generated landslide susceptibility maps play a crucial role in disaster risk management, infrastructure planning in high-risk zones, and early warning systems, supporting sustainable land-use planning. This study provides a scientific foundation for decision-making, aiding in reducing landslide-related risks in mountainous regions such as Kullu District, Himachal Pradesh.

12.2 FUTURE FOCUS

The performance comparison of Frequency Ratio (FR), Shannon Entropy (SE), and Analytical Hierarchy Process (AHP) has been successfully completed, showing that statistical models (FR and SE) outperform AHP in landslide susceptibility mapping. Future research can focus on integrating machine learning techniques like Random Forest, Support Vector Machines, and Deep Learning to enhance prediction accuracy.

Additionally, incorporating environmental factors such as soil moisture, vegetation index, and rainfall variability can improve model precision.

Further advancements can include hybrid models combining statistical, analytical, and machine learning approaches for more reliable susceptibility mapping. Temporal analysis of landslides can help assess changes over time, while field validation will ensure models align with real-world conditions. These improvements will lead to more adaptive and data-driven models, strengthening disaster preparedness and risk mitigation strategies in landslide-prone area.

REFERENCES

- **Badavath, N., Sahoo, S., & Samal, R. (2024).** Landslide susceptibility mapping for West-Jaintia Hills district, Meghalaya. *Sāadhanā*, 49(1), 52.
- **Chen, W., Guo, C., Lin, F., Zhao, R., Li, T., Tsangaratos, P., & Ilia, I. (2024).** Exploring advanced machine learning techniques for landslide susceptibility mapping in Yanchuan County, China. *Earth Science Informatics*, 1-18.
- **Chen, Z., Tang, J., & Song, D. (2024).** Modeling landslide susceptibility using alternating decision tree and support vector. *Terrestrial, Atmospheric and Oceanic Sciences*, 35(1), 12.
- **Dorji, L., & Sarkar, R. (2024).** An Evaluation of Hydrological Modeling Using CN Method and Satellite Images in Ungauged Barsa River Basin of Pasakha, Bhutan. In *Geomorphic Risk Reduction Using Geospatial Methods and Tools* (pp. 205-218). Singapore: Springer Nature Singapore.
- **Gayen, A., & Haque, S. M. (2024).** Gully Erosion Susceptibility Using Advanced Machine Learning Method in Pathro River Basin, India. In *Geomorphic Risk Reduction Using Geospatial Methods and Tools* (pp. 27-39). Singapore: Springer Nature Singapore.
- **Ha, H., Bui, Q. D., Tran, D. T., Nguyen, D. Q., Bui, H. X., & Luu, C. (2024).** Improving the forecast performance of landslide susceptibility

mapping by using ensemble gradient boosting algorithms. *Environment, Development and Sustainability*, 1-35.

- **Khatun, S., Saha, A., Gogoi, P., Saha, S., & Sarkar, R. (2024).** Assessment of Landslide Vulnerability Using Statistical and Machine Learning Methods in Bageshwar District of Uttarakhand, India. In *Geomorphic Risk Reduction Using Geospatial Methods and Tools* (pp. 99-116). Singapore: Springer Nature Singapore.
- **Lau, R., Seguí, C., Waterman, T., Chaney, N., & Veveakis, M. (2024).** Quantitative Assessment of Interferometric Synthetic Aperture Radar (INSAR) for Landslide Monitoring and Mitigation. In *Geomorphic Risk Reduction Using Geospatial Methods and Tools* (pp. 155-168). Singapore: Springer Nature Singapore.
- **Li, J., He, W., Qiu, L., Zeng, W., & Di, B. (2024).** Landslide Susceptibility Assessment Based on Machine Learning Techniques. In *Geomorphic Risk Reduction Using Geospatial Methods and Tools* (pp. 3-26). Singapore: Springer Nature Singapore.
- **Li, J., He, W., Qiu, L., Zeng, W., & Di, B. (2024).** Landslide Susceptibility Assessment Based on Machine Learning Techniques. In *Geomorphic Risk Reduction Using Geospatial Methods and Tools* (pp. 3-26). Singapore: Springer Nature Singapore.
- **Pal, S., Saha, A., Gogoi, P., & Saha, S. (2024).** An Ensemble of J48 Decision Tree with AdaBoost and Bagging for Flood Susceptibility Mapping in the Sundarbans of West Bengal, India. In *Geomorphic Risk Reduction Using Geospatial Methods and Tools* (pp. 117-133). Singapore: Springer Nature Singapore.

- **Paul, G. C., & Saha, S. (2024).** Assessment of Mouza Level Flood Resilience in Lower Part of Mayurakshi River Basin, Eastern India. In *Geomorphic Risk Reduction Using Geospatial Methods and Tools* (pp. 291-307). Singapore: Springer Nature Singapore.
- **Reddy, N. D. K., Gupta, A. K., & Sahu, A. K. (2024).** The Adoption of Random Forest (RF) and Support Vector Machine (SVM) with Cat Swarm Optimization (CSO) to Predict the Soil Liquefaction. In *Geomorphic Risk Reduction Using Geospatial Methods and Tools* (pp. 309-325). Singapore: Springer Nature Singapore.
- **Roy, B., Gogoi, P., & Saha, S. (2024).** Assessing the Shifting of the River Ganga Along Malda District of West Bengal, India Using Temporal Satellite Images. In *Geomorphic Risk Reduction Using Geospatial Methods and Tools* (pp. 193-203). Singapore: Springer Nature Singapore.
- **Saha, A., Roy, B., Saha, S., Chaudhary, A., & Sarkar, R. (2024).** An Advanced Hybrid Machine Learning Technique for Assessing the Susceptibility to Landslides in the Upper Meenachil River Basin of Kerala, India. In *Geomorphic Risk Reduction Using Geospatial Methods and Tools* (pp. 61-77). Singapore: Springer Nature Singapore.
- **Saha, S., Saha, A., Agarwal, A., Kumar, A., & Sarkar, R. (2024).** Spatial Flash Flood Modeling in the Beas River Basin of Himachal Pradesh, India, Using GIS-Based Machine Learning Algorithms. In *Geomorphic Risk Reduction Using Geospatial Methods and Tools* (pp. 135-151). Singapore: Springer Nature Singapore.
- **Saha, S., Saha, A., Roy, B., Chaudhary, A., & Sarkar, R. (2024).** Artificial Neural Network Ensemble with General Linear Model for Modeling the Landslide Susceptibility in Mirik Region of West Bengal,

India. In *Geomorphic Risk Reduction Using Geospatial Methods and Tools* (pp. 41-59). Singapore: Springer Nature Singapore.

- **Saha, S., Saha, A., Sarkar, R., Mukherjee, K., Bhardwaj, D., & Kumar, A. (2024).** Measuring Landslide Susceptibility in Jakholi Region of Garhwal Himalaya Using Landsat Images and Ensembles of Statistical and Machine Learning Algorithms. In *Geomorphic Risk Reduction Using Geospatial Methods and Tools* (pp. 219-249). Singapore: Springer Nature Singapore.
- **Sameen, M. I., Sarkar, R., Pradhan, B., Drukpa, D., Alamri, A. M., & Park, H. J. (2020).** Landslide spatial modelling using unsupervised factor optimisation and regularised greedy forests. *Computers & Geosciences*, 134, 104336.
- **Sarkar, R., Sujeewon, B. C., & Pawar, A. (2024).** Landslide Susceptibility Mapping Using Satellite Images and GIS-Based Statistical Approaches in Part of Kullu District, Himachal Pradesh, India. In *Geomorphic Risk Reduction Using Geospatial Methods and Tools* (pp. 251-287). Singapore: Springer Nature Singapore.
- **Sharma, A., & Prakash, C. (2023).** Impact assessment of road construction on landslide susceptibility in mountainous region using GIS-based statistical modelling. *Journal of the Geological Society of India*, 99(8), 1131-1140.
- **Thapa, R., Sarkar, R., Gupta, S., Kaur, H., & Alam, N. (2024).** Geospatial Study of River Shifting and Erosion–Deposition Phenomenon Along a Selected Stretch of River Damodar, West Bengal, India. In *Geomorphic Risk Reduction Using Geospatial Methods and Tools* (pp.

169-192). Singapore: Springer Nature Singapore.

- **Wei, Y., Qiu, H., Liu, Z., Huangfu, W., Zhu, Y., Liu, Y., ... & Kamp, U. (2024).** Refined and dynamic susceptibility assessment of landslides using InSAR and machine learning models. *Geoscience Frontiers*, 15(6), 101890.

PUBLICATIONS

1) International Conference on Geological and Environmental Sustainability

Sagar, D., Sharma, S., & Sarkar, R. A Comparative Study Of Empirical, Statistical, And Analytical Models For Landslide Susceptibility In Kullu District, Himachal Pradesh. International Conference on Geological and Environmental Sustainability (ICGES-25), 03rd-May-2025, Chandigarh, India





2) International Conference on Interdisciplinary Academic Research and Innovation (IARI-25)

Sagar, D., & Sarkar, R. Empirical Modelling of Landslide Susceptibility in Kullu District Using Frequency Ratio and GIS. International Conference on Interdisciplinary Academic Research and Innovation (IARI-25) 18th May 2025 Agra, India



The image is a formal acceptance letter from the Society for Education (SFE) for the International Conference on Interdisciplinary Academic Research and Innovation (IARI-25). The letter is dated 18th May 2025 and is addressed to the author, Dhiren Sagar, Raju Sarkar. It congratulates the author for having their paper, 'Empirical Modelling of Landslide Susceptibility in Kullu District Using Frequency Ratio and GIS Integration', accepted for publication and oral presentation at the conference. The letter also provides the registration link: <https://www.sfe.net.in/conf/registration.php?id=3337742> and invites the author to present their paper at the conference. The letter is signed by Dr. James Crusoe, President of SFE, and includes the SFE logo and contact information.

SFE
SOCIETY FOR EDUCATION

International Conference on Interdisciplinary Academic Research and Innovation - IARI-25

18th May 2025 | Agra

Acceptance Letter

Paper ID: SFE_62709

Paper Title: Empirical Modelling of Landslide Susceptibility in Kullu District Using Frequency Ratio and GIS Integration

Authors Name: Dhiren Sagar, Raju Sarkar

Dear Author,

With heartiest congratulations I am pleased to inform you that based on the recommendations of the reviewers and the Technical Program Committees, your paper identified above has been accepted for publication and oral presentation by **International Conference on Interdisciplinary Academic Research and Innovation - IARI-25**.

This conference received number of submissions from different countries and regions, reviewed by international experts and your paper cleared all the criteria, got accepted for the conference. Your paper will be published in the conference proceeding after the registration.

For registration: <https://www.sfe.net.in/conf/registration.php?id=3337742>

Herewith, the conference committee sincerely invites you to come to present your paper at our conference.

Sincerely,


Dr. James Crusoe
President
Society for Education (SFE)



+91 9677007228 info@sfe.net.in www.sfe.net.in



CERTIFICATE OF PRESENTATION



International Conference on Interdisciplinary Academic Research and Innovation(IARI-25)

18th May 2025 | Agra - India

This is to certify that.....**Dhiren Sagar**.....affiliated with
.....Delhi Technological University, Delhi, India.....has presented a paper titled

.....Empirical Modelling of Landslide Susceptibility in Kullu District Using Frequency Ratio and GIS Integration.....

.....
at the conference organized by the Society For Education (SFE) held on 18th May 2025 at Agra - India.




Dr. James Crusoe
President, SFE




Shradha Srinath
Convener



